Supporting Information

Pyrrolo-[3,2-*b*]pyrroles for photochromic analysis of halocarbons

Jia-Ying Wu,[a] Cheng-Han Yu,[b] Jung-Jung Wen,[b] Chiou-Ling Chang,[b] Man-kit Leung[a,b,*]

[a] *Institute of Polymer Science and Engineering, National Taiwan University, Taipei 106, Taiwan, ROC*

[b] *Department of Chemistry, National Taiwan University, Taipei 106, Taiwan, ROC*

Email. mkleung@ntu.edu.tw

Table of content S1
Experimental Section S3
X-ray crystallographic analysis. S12
Cylic voltammetry and differential pulse voltammetry studies 1-4 and TPA S34
Preliminary studies of photochromic response of 1 in the presence of various halocarbons S39
Time resolved photochromic studies. S41
Preliminary studies of the PET mechanisms. S48
References S51
Figure S1. ^{1}H NMR Spectrum of **3** S6
Figure S2. ^{13}C NMR Spectrum of **3** S7
Figure S3. ^{1}H NMR Spectrum of **4** S8
Figure S4. ^{13}C NMR Spectrum of **4** S9
Figure S5.^{1}H NMR Spectrum of **1** S10
Figure S6.^{1}H NMR Spectrum of **2** S11
Figure S7. The ORTEP of **3** and X-ray crystal parameters, bond lengths and bond angles S13
Figure S8. The ORTEP of **4** and X-ray crystal parameters, bond lengths and bond angles S21
Figure S9. The ORTEP of **1** and X-ray crystal parameters, bond lengths and bond angles S26
Figure S10 CV and DPV of TPA. S35
Figure S11 CV and DPV of **4.** S36
Figure S12 CV and DPV of **3**. S36
Figure S13 CV and DPV of **1**. S37
Figure S14 CV and DPV of **2**. S37
Table S1. Photophysical properties of DHPP and TPA S38
Figure S15. Photochromic responses of **1** (1×10^{-5}) with additional halocarbons other than those reported in the article indeed have been tested. S40
Figure S16. Time resolved photochromic change of **1** in pure Toluene and in the presence of CH_2Cl_2 in toluene S42
Figure S17. Time resolved photochromic change of **1** in the presence of CCl_4 in toluene S43
Figure S18. Time resolved photochromic change of **1** in the presence of $Br(CH_2)_2Br$ in toluene S44
Figure S19. Time resolved photochromic change of **1** in the presence of $Br_2CHCHBr_2$ in toluene S45
Figure S20. Time resolved photochromic change of **1** in the presence of $CHBr_3$ in toluene S46

Figure S21. Time resolved photochromic change of **1** in the presence of CH_2I_2 in toluene S47
Figure S22. Spectroelectrochemical analyses of $\mathbf{1}^{(\cdot+)}$ (left) and $\mathbf{2}^{(\cdot+)}$ (right) in CH_2Cl_2, using TBAP (0.1 M) as the supporting electrolyte. S48
Figure S23. Time resolved photochromic change of **1** in the presence of $CHCl_3$ in toluene. S49
Figure S24. Photochromic change of **1** or **2** in $CHCl_3$ and in CH_2Cl_2 in the presence of Bu_4NClO_4. S50
Quantitative Analysis of $CHCl_3$ and CH_2Cl_2 Contents. S51
Figure S25. The cell for detection of the photochromatic change. S51
Figure S26. Photochromatic change of DHPP**1** (0.001 M) in CH_3CN/toluene (2:1) in the presence of $CHCl_3$ with the sample concentration of: (a) blank, (b) 0.001 M, (c) 0.005 M, (d) 0.01M, (e) 0.05 M, (f) 0.1M. Note that the samples were diluted by 10 times before measurement. S52
Figure S27. Photochromatic change of DHPP**1** (0.001 M) in CH_3CN/toluene (2:1) in the presence of various amounts of CH_2Cl_2: (a) 12.5 V/V%; (b) 25 V/V%; (c) 50 V/V%. S54
Figure S28. Linear plots of the absorbance change against irradiation time in the presence of various concentrations of CH_2Cl_2. The slope of each line represents the rate of photochromic change. Inset is the plot of the plot of rate of photochromic change versus [CH_2Cl_2]. The observation of the linear behavior suggests a pseudo first order kinetics for [CH_2Cl_2]. S55

Table S1. Essential structural information (in Å) about the DHPP core of 1, 3, and 4 S12
Table S2. Crystal data and Structure refinement for 3 (number ic16812) S14
Table S3. Atomic coordinates for 3 (number ic16812) S15
Table S4. Bond lengths and angles for 3 (number ic16812) S16
Table S5. Anisotropic displacement parameters for 3 (number ic16812) S13
Table S6. Crystal data and Structure refinement for 4 (number ic16830) S22
Table S7. Atomic coordinates for 4 (number ic16830) S23
Table S8. Bond lengths and angles for 4 (number ic16830) S24
Table S9. Anisotropic displacement parameters for 4 (number ic16830) S25
Table S10. Crystal data and Structure refinement for 1 (number ic 17293) S26
Table S11. Atomic coordinates for 1 (number ic17293) S28
Table S12. Bond lengths and angles for 1 (number ic17293) S30
Table S13. Anisotropic displacement parameters for 1 (number ic17293) S32
Table S14. Photophysical properties of DHPP 1-4 and Triphenylamine S38

Materials. All reagents, including 2,3-butanedione, ammonium acetate, benzaldehyde, aniline, 4-(diphenylamino)benzaldehyde and acetic acid were commercially available. Ethanol was dried by molecular sieves and distilled before use.

Synthesis

4,4'-(2,5-Diphenylpyrrolo[3,2-b]pyrrole-1,4-diyl)bis(N,N-diphenylaniline) (**3**). 2,3-Butanedione (1.12 g, 13.0 mmol), NH_4OAc（7.00 g, 91.0 mmol), benzaldehyde (1.38 g, 13.00 mmol) and *N*',*N*'-diphenylbenzene-1,4-diamine (3.38 g, 13.0 mmol)[1] were placed in two-necked flask (500 mL) equipped with a magnetic stirring bar. Acetic acid (198.0 mL) were injected into the flask and the mixture was allowed to reflux at 120 °C for 3 hrs. The mixture was cooled and precipitated into water. The grey black precipitate was filtered, purified by chromatography on silica gel by using chloroform/hexane 2:1 as eluent, and recrystallized from CH_2Cl_2/CH_3OH to get **1** as white solid (0.55 g, 15%). m.p. 249℃; ^{1}H NMR (400 MHz, $CDCl_3$) δ 6.41 (s, 2H), 6.99-7.05 (m, 9H), 7.10-7.19 (m, 15 H), 7.24-7.28 (m, 14 H); ^{13}C NMR (100 MHz, $CDCl_3$) δ 94.35, 122.90, 124.04, 124.29, 126.02, 126.10, 128.08, 128.17, 129.27, 131.53, 133.73, 134.58, 135.83, 145.43, 147.62. HRMS (ESI) calcd for $C_{54}H_{41}N_4$ 745.3326, obsd. 745.3317 (M^+ + H). Anal. calcd for $C_{54}H_{40}N_4$: C, 87.07; H, 5.41; N, 7.52; found C, 86.86; H, 5.18; N, 7.59.

1,2,4,5-Tetraphenyl-1,4-dihydropyrrolo[3,2-b]pyrrole (**4**). 2,3-Butanedione (1.12 g, 13.0 mmol), NH_4OAc（7.00 g, 91.1 mmol), benzaldehyde (1.38 g, 13.0 mmol) and aniline (1.21 g, 13.0 mmol) were placed in two-necked flask (500 mL) equipped with a magnetic stirring bar. Acetic acid (198.0 mL) were injected and refluxed at 120 °C for 3 hrs. The mixture was cooled and precipitated into water. The yellow precipitate was filtered and recrystallized by dichloromethane/ hexane to get **12** as light yellow solid (0.55 g, 15%). m.p. 286℃; ^{1}H NMR

(400 MHz, d_6-DMSO) δ 6.44-6.45 (s, 2H), 7.16-7.19 (m, 6H), 7.23-7.30 (m, 10H), 7.40-7.44 (t, *J*= 7.43 Hz, 2H); ^{13}C NMR (100 MHz, $CDCl_3$) δ 94.87, 125.07, 125.47, 126.02, 128.01, 128.05, 128.92, 131.41, 133.50, 135.63, 139.87. HRMS (ESI) calcd for $C_{30}H_{22}N_2$ 410.1778 (M^+), obsd. 410.1770 Anal. calcd for $C_{30}H_{22}N_2$: C, 87.77; H, 5.40; N, 6.82; found C, 87.56; H, 5.18; N, 6.88.

4,4'-(1,4-diphenyl-1,4-dihydropyrrolo[3,2-b]pyrrole-2,5-diyl)bis(N,N-diphenylaniline) (**1**)
Aniline (1.23 g, 13.2 mmole), 4-(diphenylamino)benzaldehyde (3.00 g, 11.0 mmole) and ethanol (30 mL) were added to a two-necked flask (100 mL) under nitrogen atmosphere and refluxed at 80 °C for 24 hours. After cooling, 2,3-butanedione (0.47g, 5.5 mmole) and acetic acid (15mL) were injected and allowed to react in ambient temperature for 72 hours. After the reaction was finished, the reaction mixture was neutralized with saturated aqueous NaOH in an ice bath. The product was extracted with CH_2Cl_2 twice. The combined extract was dried with anhydrous $MgSO_4$, filtered, and concentrated under reduced pressure to give a crude product that was purified by liquid column chromatography on silica gel, using CH_2Cl_2/hexane (1:2) as the eluent, followed by recrystallized from toluene/ether to afford **1** (1.07 g, 26%) ^{1}H NMR (400 MHz, d_6-DMSO) δ 6.38 (s, 2H), 6.83 (d, *J* = 8.68 Hz, 4H), 6.97-7.04 (m, 10H), 7.08 (d, *J* = 8.68 Hz, 4H), 7.26-7.41 (m, 14H), 7.43 (t, *J* = 7.40 Hz, 4H); MS (ESI) calcd for $C_{54}H_{40}N_4$: 744.92; found 744.32 (M^+); Anal. calcd for $C_{54}H_{40}N_4$: C, 87.07; H, 5.41; N, 7.52; found C, 86.87; H, 5.62; N, 7.54.

4,4'-(1,4-diphenyl-1,4-dihydropyrrolo[3,2-b]pyrrole-2,5-diyl)bis(N,N-di-4-tolylaniline) (**2**). Similar procedure from *N',N'*-di(*p*-tolyl)benzene-1,4-diamine [2] as described for **1** was carried to obtain **2** in 22% yields. ^{1}H NMR (400 MHz, CD_2Cl_2) δ 2.30 (bs, 12H), 6.82 (d, *J* = 8.0 Hz, 4H), 6.97-7.20 (broad peaks, 22H), 7.25 (t, *J* = 8 Hz, 2H), 7.25 (d, *J* = 8 Hz, 4H), 7.8 (t, *J* = 8 Hz, 4H); MS (ESI) calcd for $C_{58}H_{48}N_4$: 801.03; found 801.39 (M^+); Anal. calcd for $C_{58}H_{48}N_4$: C, 86.97; H, 6.04; N, 6.99 ; found C, 87.03; H, 6.37; N, 6.90.

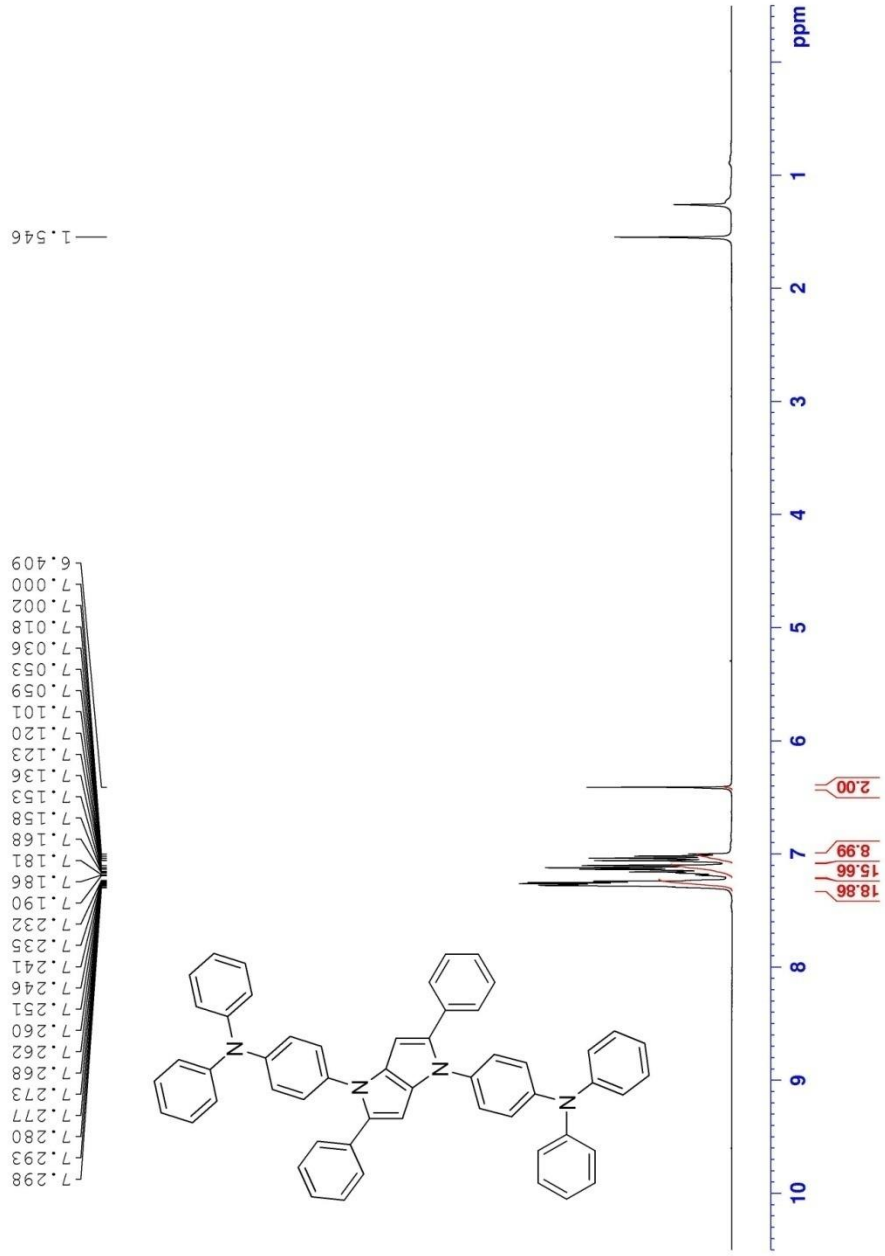

Figure S1 ^{1}H NMR spectrum of **3**

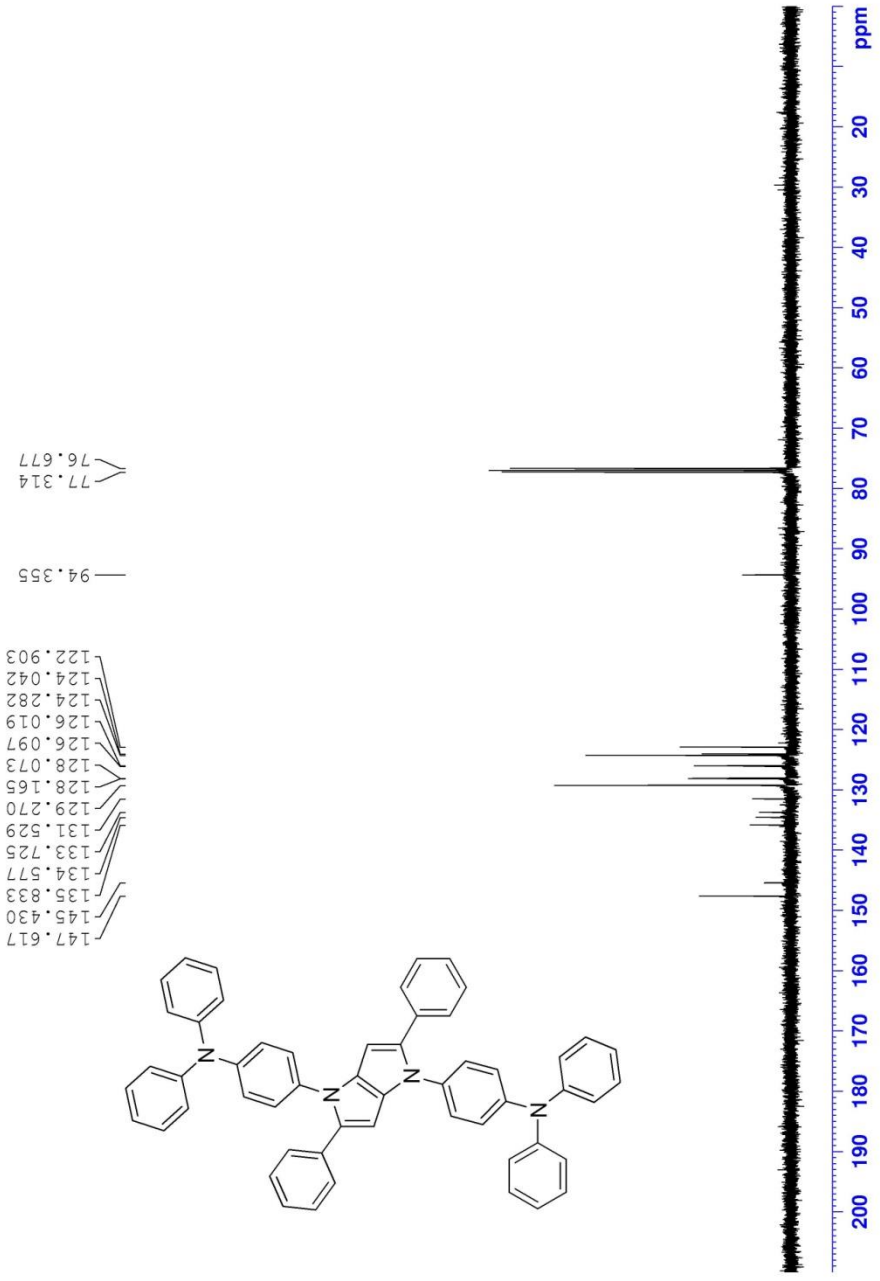

Figure S2 ^{13}C NMR spectrum of **3**

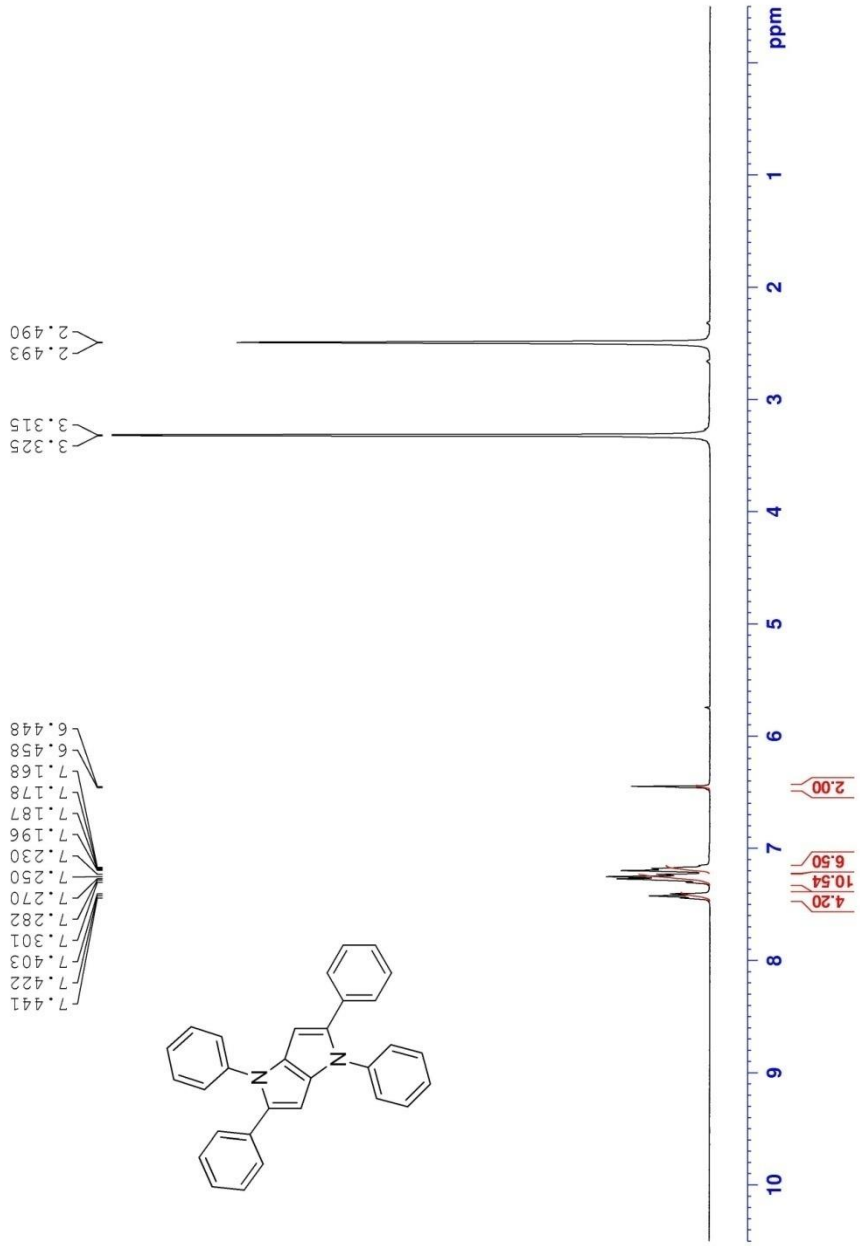

Figure S3 ^{1}H NMR spectrum of **4**

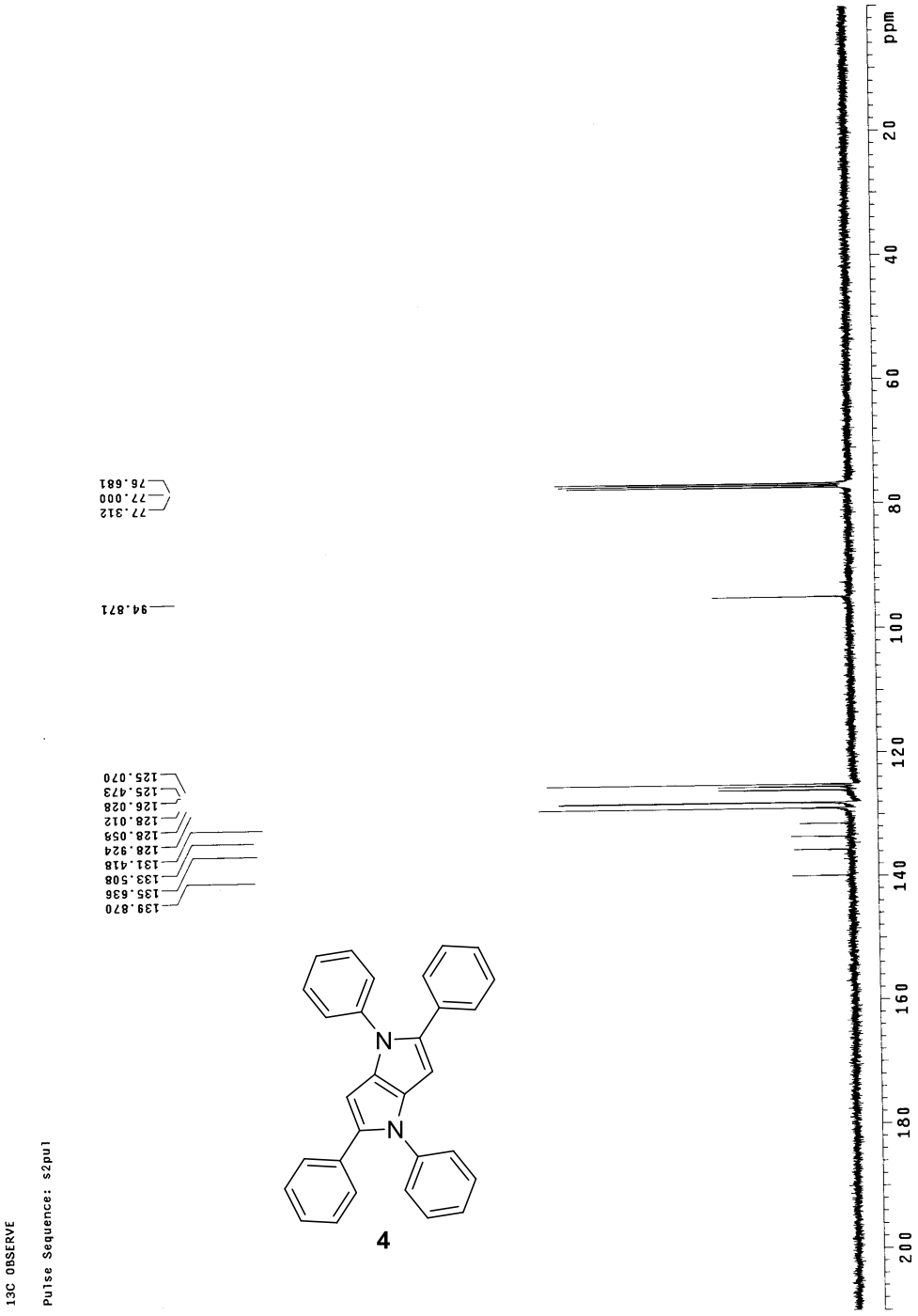

Figure S4 ^{13}C NMR spectrum of **4**

Figure S5 ^{1}H NMR spectrum of **1**

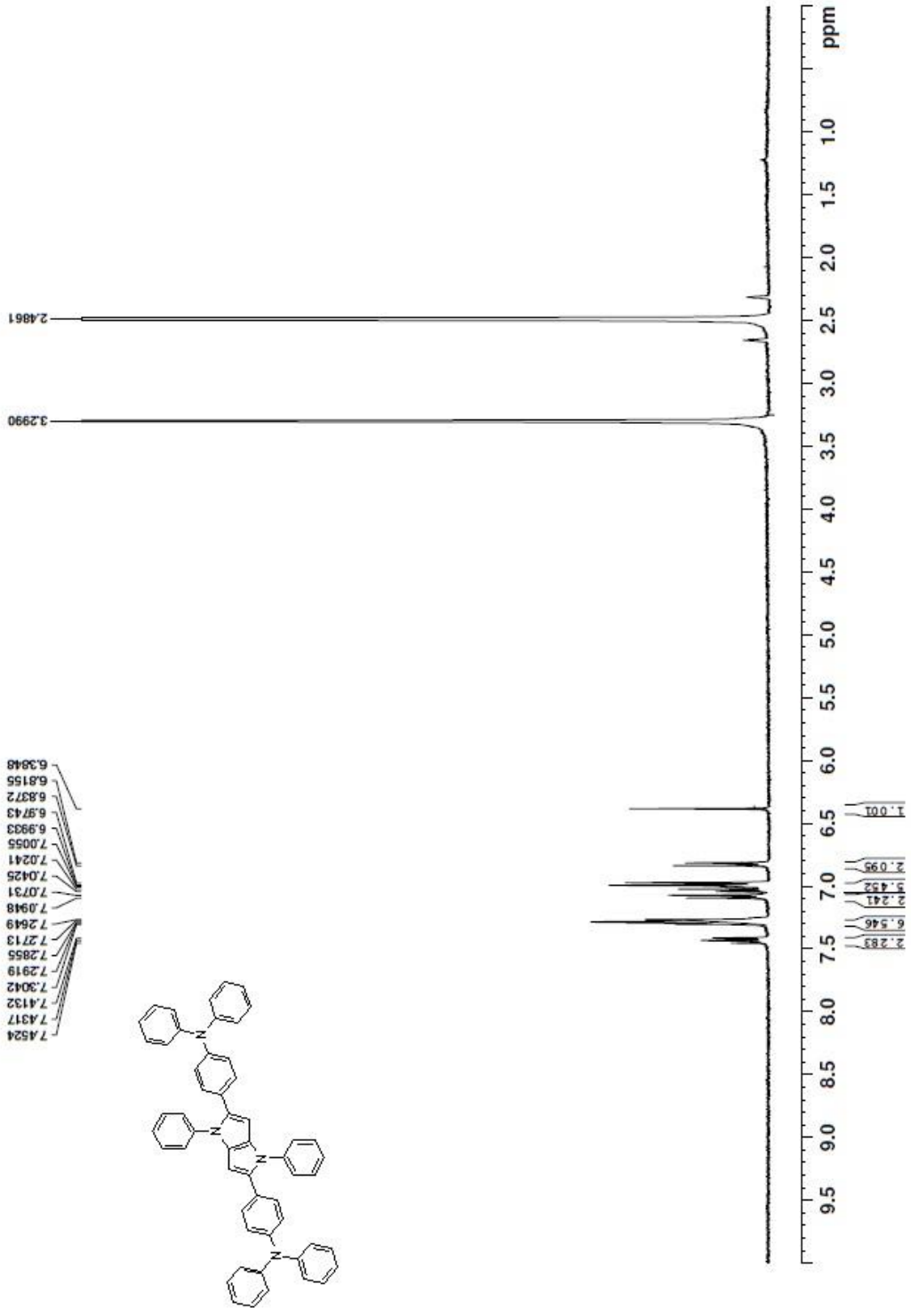
2.4861
3.2990
6.3848
6.8155
6.8372
6.9743
6.9933
7.0055
7.0241
7.0425
7.0731
7.0948
7.2649
7.2713
7.2855
7.2919
7.3042
7.4132
7.4317
7.4524
1.001
2.095
5.452
2.241
6.546
2.283
ppm

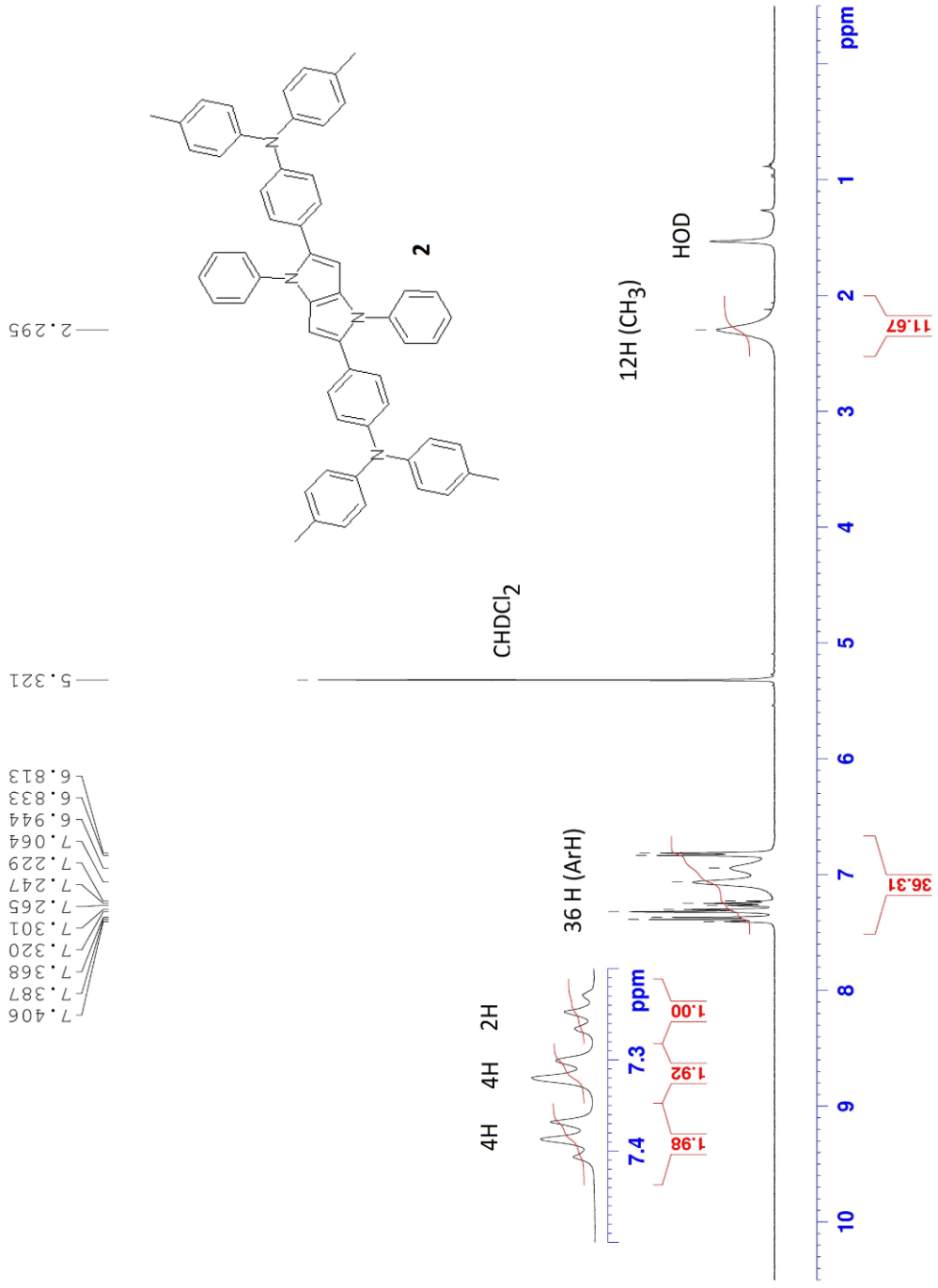

Figure S6 ^{1}H NMR spectrum of **2**

X-ray crystallographic analysis.

Preparation of single crystals: Single crystal of **1** obtained from slow evaporation of the organic solvents from a toluene-ether solution while crystals of **3** and **4** were prepared from $CHCl_3$. The ORTEPs are shown in Figures S7 to S9. The atomic coordination data are listed below. The CIF files are attached in the SI.

Structural Information. The average DHPP C-C bond length is 1.39 ± 0.02 Å. The small deviation of the C-C bond length indicates strong aromaticity in the DHPP core. Although observation of the relatively short C_a–C_b/$C_{a'}$–$C_{b'}$ bond of 1.355 Å and long C_b–C_c/$C_{b'}$–$C_{c'}$ bond of 1.410 Å in **4** suggests that some degree of bond alternation in the DHPP core, bond alternation is reduced by introducing the $(Ph)_2NC_6H_4$- moieties either to the *N,N'*-positions or 2,5-positions in **1** and **3**.

Table S1. Essential structural information (in Å) about the DHPP core of 1, 3, and 4

DHPP	N–C_a	N'–$C_{a'}$	C_a–C_b	$C_{a'}$–$C_{b'}$	C_b–C_c	$C_{b'}$–$C_{c'}$	C_c– $C_{c'}$	N–C_c	N'–$C_{c'}$
1	1.397	1.404	1.387	1.382	1.405	1.394	1.370	1.397	1.391
3	1.401	1.386	1.387	1.388	1.391	1.404	1.398	1.377	1.400
4	1.410	1.410	1.355	1.355	1.410	1.410	1.390	1.375	1.375

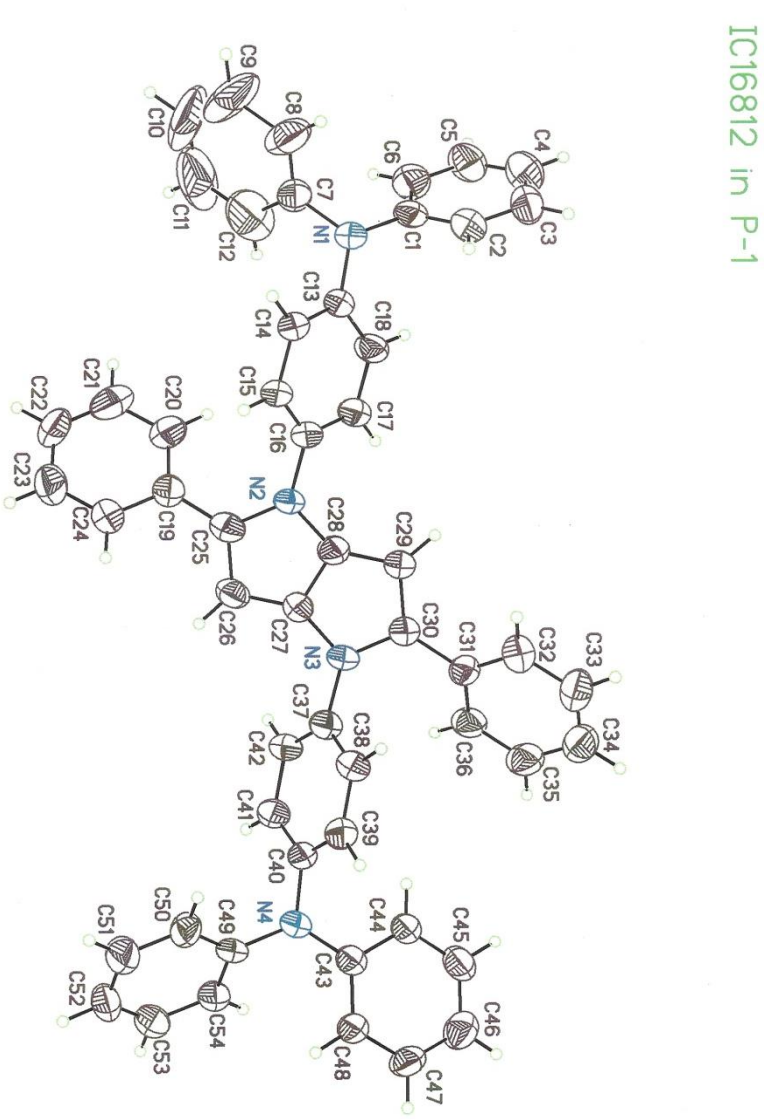

Figure S7. The ORTEP of **3**

Table S2. Crystal data and Structure refinement for 3 (number ic16812)

Identification code	ic16812
Empirical formula	$C_{54}H_{40}N_4$
Formula weight	744.90
Temperature	200(2) K
Wavelength	1.54178 Å
Crystal system	Triclinic
Space group	$P\bar{1}$
Unit cell dimensions	a = 10.5757(18) Å alpha = 97.350(14)° b = 13.339(2) Å beta = 106.509(15)° c = 15.978(3) Å gamma = 107.809(16)°
Volume, Z	1999.8(6) $Å^3$, 2
Density (calculated)	1.237 Mg/m^3
Absorption coefficient	0.557 mm^{-1}
F(000)	784
Crystal size	0.20 x 0.15 x 0.10 mm
Θ range for data collection	3.58 to 67.99°
Limiting indices	$-12 \le h \le 12$, $-14 \le k \le 16$, $-19 \le l \le 14$
Reflections collected	10987
Independent reflections	7173 (R_{int} = 0.1355)
Completeness to Θ = 67.99°	98.4 %
Absorption correction	Semi-empirical from equivalents
Max. and min. transmission	1.00000 and 0.91056
Refinement method	Full-matrix least-squares on F^2
Data / restraints / parameters	7173 / 0 / 524
Goodness-of-fit on F^2	0.908
Final R indices [I>2σ(I)]	R1 = 0.0844, wR2 = 0.2282
R indices (all data)	R1 = 0.2052, wR2 = 0.3529
Extinction coefficient	0.0005(2)
Largest diff. peak and hole	0.307 and -0.219 $eÅ^{-3}$

Table S3. Atomic coordinates for 3 (number ic16812)

Atomic coordinates [x 10^4] and equivalent isotropic displacement parameters [$Å^2$ x 10^3] for ic16812. U(eq) is defined as one third of the trace of the orthogonalized U_{ij} tensor.

	x	y	z	U(eq)
N(1)	4751(6)	5402(5)	7734(4)	51(1)
N(2)	5990(6)	7576(5)	5104(4)	47(1)
N(3)	4993(6)	8988(5)	3538(4)	47(1)
N(4)	6154(6)	11536(5)	1120(4)	56(2)
C(1)	3335(7)	4837(5)	7669(5)	49(2)
C(2)	2479(8)	5404(6)	7759(5)	56(2)
C(3)	1096(9)	4864(7)	7699(6)	71(2)
C(4)	593(9)	3746(8)	7568(7)	84(3)
C(5)	1453(9)	3177(7)	7464(6)	73(2)
C(6)	2826(9)	3714(6)	7527(6)	66(2)
C(7)	5813(8)	4988(7)	8145(6)	66(2)
C(8)	6237(10)	5107(8)	9048(7)	87(3)
C(9)	7281(13)	4688(13)	9436(13)	173(10)
C(10)	7864(14)	4220(18)	8959(19)	232(16)
C(11)	7386(19)	4081(16)	8003(18)	217(13)
C(12)	6367(16)	4479(11)	7624(11)	137(6)
C(13)	5011(7)	6006(5)	7097(5)	46(2)
C(14)	6262(7)	6855(6)	7305(5)	48(2)
C(15)	6604(7)	7402(5)	6663(5)	47(2)
C(16)	5659(7)	7084(5)	5799(5)	48(2)
C(17)	4359(7)	6284(6)	5585(5)	56(2)
C(18)	4010(7)	5747(6)	6227(5)	53(2)
C(19)	8336(7)	7354(6)	5232(5)	51(2)
C(20)	8112(8)	6390(6)	5523(5)	58(2)
C(21)	9204(10)	6017(8)	5812(5)	73(2)
C(22)	10512(9)	6562(8)	5816(6)	76(2)
C(23)	10800(9)	7542(9)	5563(6)	77(3)
C(24)	9717(8)	7909(7)	5261(6)	64(2)
C(25)	7216(8)	7771(6)	4878(5)	53(2)
C(26)	7133(7)	8352(5)	4216(5)	50(2)
C(27)	5847(7)	8504(5)	4043(4)	46(1)
C(28)	5120(7)	8006(6)	4574(4)	50(2)
C(29)	3853(7)	8204(6)	4421(5)	53(2)
C(30)	3799(7)	8814(6)	3782(5)	50(2)
C(31)	2622(6)	9155(5)	3346(4)	46(1)
C(32)	1918(8)	9523(6)	3854(5)	58(2)
C(33)	807(8)	9830(6)	3452(6)	62(2)
C(34)	380(8)	9829(6)	2557(6)	67(2)
C(35)	1094(8)	9459(7)	2028(6)	66(2)
C(36)	2192(7)	9107(6)	2425(5)	56(2)
C(37)	5429(7)	9693(5)	2982(4)	48(2)
C(38)	5303(7)	10694(5)	3083(5)	48(2)
C(39)	5598(7)	11333(5)	2492(5)	49(2)
C(40)	5997(7)	10928(6)	1791(5)	51(2)
C(41)	6209(8)	9974(6)	1731(5)	55(2)
C(42)	5896(7)	9316(5)	2330(5)	50(2)
C(43)	4972(7)	11712(6)	584(5)	49(2)
C(44)	3610(7)	11066(6)	514(5)	51(2)

C(45)	2439(8)	11223(6)	-22(5)	60(2)
C(46)	2571(8)	12012(7)	-512(6)	66(2)
C(47)	3915(8)	12654(6)	-417(5)	60(2)
C(48)	5101(7)	12521(6)	110(5)	54(2)
C(49)	7508(7)	11893(5)	1019(5)	50(2)
C(50)	8728(7)	12275(7)	1781(5)	56(2)
C(51)	10040(9)	12628(8)	1707(6)	75(3)
C(52)	10179(8)	12627(8)	872(6)	68(2)
C(53)	8977(8)	12231(6)	106(5)	59(2)
C(54)	7640(8)	11865(6)	174(5)	54(2)

Table S4. Bond lengths and angles for 3 (number ic16812)

Bond lengths [Å] and angles [°] for ic16812.

N(1)-C(13)	1.414(7)	N(1)-C(1)	1.421(8)
N(1)-C(7)	1.431(9)	N(2)-C(28)	1.377(8)
N(2)-C(25)	1.401(9)	N(2)-C(16)	1.433(7)
N(3)-C(30)	1.386(8)	N(3)-C(27)	1.400(8)
N(3)-C(37)	1.438(7)	N(4)-C(43)	1.405(8)
N(4)-C(49)	1.427(8)	N(4)-C(40)	1.441(7)
C(1)-C(2)	1.371(10)	C(1)-C(6)	1.391(10)
C(2)-C(3)	1.388(10)	C(3)-C(4)	1.387(13)
C(4)-C(5)	1.381(13)	C(5)-C(6)	1.376(11)
C(7)-C(8)	1.357(13)	C(7)-C(12)	1.367(15)
C(8)-C(9)	1.410(15)	C(9)-C(10)	1.32(3)
C(10)-C(11)	1.43(3)	C(11)-C(12)	1.368(17)
C(13)-C(14)	1.371(9)	C(13)-C(18)	1.411(9)
C(14)-C(15)	1.400(8)	C(15)-C(16)	1.375(10)
C(16)-C(17)	1.374(10)	C(17)-C(18)	1.394(8)
C(19)-C(20)	1.398(10)	C(19)-C(24)	1.405(10)
C(19)-C(25)	1.462(10)	C(20)-C(21)	1.379(11)
C(21)-C(22)	1.349(13)	C(22)-C(23)	1.388(13)
C(23)-C(24)	1.368(11)	C(25)-C(26)	1.387(9)
C(26)-C(27)	1.391(9)	C(27)-C(28)	1.398(8)
C(28)-C(29)	1.404(9)	C(29)-C(30)	1.385(9)
C(30)-C(31)	1.475(8)	C(31)-C(32)	1.385(10)
C(31)-C(36)	1.397(9)	C(32)-C(33)	1.376(10)
C(33)-C(34)	1.371(11)	C(34)-C(35)	1.419(12)
C(35)-C(36)	1.401(10)	C(37)-C(42)	1.376(10)
C(37)-C(38)	1.376(10)	C(38)-C(39)	1.389(9)
C(39)-C(40)	1.405(10)	C(40)-C(41)	1.355(10)
C(41)-C(42)	1.419(8)	C(43)-C(48)	1.391(9)
C(43)-C(44)	1.398(9)	C(44)-C(45)	1.383(10)
C(45)-C(46)	1.387(10)	C(46)-C(47)	1.370(11)
C(47)-C(48)	1.374(9)	C(49)-C(54)	1.393(9)
C(49)-C(50)	1.398(10)	C(50)-C(51)	1.367(10)
C(51)-C(52)	1.383(11)	C(52)-C(53)	1.390(11)
C(53)-C(54)	1.388(10)		

C(13)-N(1)-C(1)	119.6(5)	C(13)-N(1)-C(7)	116.4(5)
C(1)-N(1)-C(7)	118.2(5)	C(28)-N(2)-C(25)	108.8(5)
C(28)-N(2)-C(16)	122.6(5)	C(25)-N(2)-C(16)	128.5(5)
C(30)-N(3)-C(27)	108.5(5)	C(30)-N(3)-C(37)	126.8(5)
C(27)-N(3)-C(37)	123.9(5)	C(43)-N(4)-C(49)	123.7(5)
C(43)-N(4)-C(40)	118.9(5)	C(49)-N(4)-C(40)	117.4(5)
C(2)-C(1)-C(6)	120.0(7)	C(2)-C(1)-N(1)	119.8(6)
C(6)-C(1)-N(1)	120.2(7)	C(1)-C(2)-C(3)	120.4(7)
C(4)-C(3)-C(2)	119.5(8)	C(5)-C(4)-C(3)	119.8(7)
C(6)-C(5)-C(4)	120.6(8)	C(5)-C(6)-C(1)	119.6(8)
C(8)-C(7)-C(12)	121.6(10)	C(8)-C(7)-N(1)	118.5(8)
C(12)-C(7)-N(1)	119.9(10)	C(7)-C(8)-C(9)	117.5(14)
C(10)-C(9)-C(8)	122.6(18)	C(9)-C(10)-C(11)	119.4(12)
C(12)-C(11)-C(10)	118.2(18)	C(7)-C(12)-C(11)	120.8(17)
C(14)-C(13)-C(18)	118.0(5)	C(14)-C(13)-N(1)	120.6(6)
C(18)-C(13)-N(1)	121.3(6)	C(13)-C(14)-C(15)	121.9(6)
C(16)-C(15)-C(14)	119.2(6)	C(17)-C(16)-C(15)	120.2(6)
C(17)-C(16)-N(2)	118.4(6)	C(15)-C(16)-N(2)	121.4(6)
C(16)-C(17)-C(18)	120.5(7)	C(17)-C(18)-C(13)	119.8(6)
C(20)-C(19)-C(24)	116.5(7)	C(20)-C(19)-C(25)	123.6(7)

C(24)-C(19)-C(25)	119.9(6)	C(21)-C(20)-C(19)	120.6(8)
C(22)-C(21)-C(20)	121.3(8)	C(21)-C(22)-C(23)	120.3(7)
C(24)-C(23)-C(22)	118.7(8)	C(23)-C(24)-C(19)	122.5(7)
C(26)-C(25)-N(2)	108.6(6)	C(26)-C(25)-C(19)	126.0(6)
N(2)-C(25)-C(19)	125.3(5)	C(25)-C(26)-C(27)	106.1(6)
C(26)-C(27)-C(28)	110.1(5)	C(26)-C(27)-N(3)	143.6(6)
C(28)-C(27)-N(3)	106.2(5)	N(2)-C(28)-C(27)	106.3(6)
N(2)-C(28)-C(29)	143.8(6)	C(27)-C(28)-C(29)	109.6(5)
C(30)-C(29)-C(28)	106.3(6)	C(29)-C(30)-N(3)	109.4(6)
C(29)-C(30)-C(31)	127.0(6)	N(3)-C(30)-C(31)	123.4(5)
C(32)-C(31)-C(36)	119.0(6)	C(32)-C(31)-C(30)	119.7(6)
C(36)-C(31)-C(30)	121.3(6)	C(33)-C(32)-C(31)	120.2(7)
C(34)-C(33)-C(32)	122.7(8)	C(33)-C(34)-C(35)	117.9(7)
C(36)-C(35)-C(34)	119.8(7)	C(31)-C(36)-C(35)	120.4(8)
C(42)-C(37)-C(38)	121.9(6)	C(42)-C(37)-N(3)	118.4(6)
C(38)-C(37)-N(3)	119.6(6)	C(37)-C(38)-C(39)	119.7(6)
C(38)-C(39)-C(40)	118.8(6)	C(41)-C(40)-C(39)	121.2(6)
C(41)-C(40)-N(4)	119.8(7)	C(39)-C(40)-N(4)	119.0(6)
C(40)-C(41)-C(42)	119.8(6)	C(37)-C(42)-C(41)	118.3(6)
C(48)-C(43)-C(44)	117.7(6)	C(48)-C(43)-N(4)	122.1(6)
C(44)-C(43)-N(4)	120.2(6)	C(45)-C(44)-C(43)	120.6(6)
C(44)-C(45)-C(46)	121.5(7)	C(47)-C(46)-C(45)	117.0(7)
C(46)-C(47)-C(48)	122.9(6)	C(47)-C(48)-C(43)	120.2(6)
C(54)-C(49)-C(50)	119.1(6)	C(54)-C(49)-N(4)	121.3(7)
C(50)-C(49)-N(4)	119.5(6)	C(51)-C(50)-C(49)	121.0(7)
C(50)-C(51)-C(52)	120.2(8)	C(51)-C(52)-C(53)	119.6(7)
C(54)-C(53)-C(52)	120.6(7)	C(53)-C(54)-C(49)	119.5(7)

Symmetry transformations used to generate equivalent atoms:

Table S5. Anisotropic displacement parameters for 3 (number ic16812)

Anisotropic displacement parameters [$Å^2 \times 10^3$] for ic16812.

The anisotropic displacement factor exponent takes the form:

$-2\pi^2 [(ha^*)^2 U_{11} + ... + 2hka^* b^* U_{12}]$

	U11	U22	U33	U23	U13	U12
N(1)	53(3)	69(4)	49(3)	34(3)	25(3)	30(3)
N(2)	42(3)	63(3)	44(3)	31(3)	17(2)	17(3)
N(3)	50(3)	60(3)	43(3)	29(3)	23(3)	22(3)
N(4)	46(3)	71(4)	63(4)	43(3)	26(3)	22(3)
C(1)	48(4)	49(4)	54(4)	29(3)	22(3)	12(3)
C(2)	55(4)	57(4)	60(4)	21(3)	26(4)	17(3)
C(3)	59(5)	80(5)	95(7)	39(5)	41(5)	33(4)
C(4)	52(5)	82(6)	116(8)	46(6)	36(5)	5(4)
C(5)	60(5)	68(5)	86(6)	25(4)	30(5)	7(4)
C(6)	74(5)	61(4)	76(6)	27(4)	32(5)	30(4)
C(7)	58(4)	68(5)	96(6)	56(5)	37(5)	31(4)
C(8)	63(5)	91(7)	81(6)	45(5)	-5(5)	10(5)
C(9)	75(8)	154(13)	250(20)	171(15)	-12(10)	5(8)
C(10)	66(8)	250(20)	450(40)	280(30)	68(14)	79(11)
C(11)	173(16)	230(20)	450(40)	260(30)	220(20)	168(17)
C(12)	170(14)	128(11)	227(17)	110(12)	139(13)	115(11)
C(13)	40(3)	51(3)	52(4)	26(3)	20(3)	15(3)
C(14)	44(3)	62(4)	45(4)	26(3)	16(3)	22(3)
C(15)	45(3)	53(4)	53(4)	31(3)	22(3)	19(3)
C(16)	50(4)	52(4)	53(4)	30(3)	23(3)	23(3)
C(17)	47(4)	67(4)	56(4)	32(4)	20(3)	16(3)
C(18)	43(3)	56(4)	52(4)	24(3)	15(3)	4(3)
C(19)	48(4)	62(4)	47(4)	17(3)	17(3)	21(3)
C(20)	62(4)	56(4)	58(4)	21(3)	14(4)	26(4)
C(21)	97(7)	85(6)	51(5)	23(4)	19(5)	55(5)
C(22)	61(5)	104(7)	80(6)	37(5)	19(5)	52(5)
C(23)	59(5)	116(8)	75(6)	33(5)	36(5)	41(5)
C(24)	53(4)	82(5)	74(5)	38(4)	31(4)	30(4)
C(25)	60(4)	60(4)	46(4)	20(3)	26(3)	21(3)
C(26)	58(4)	56(4)	50(4)	22(3)	31(3)	22(3)
C(27)	47(4)	56(4)	47(4)	21(3)	24(3)	24(3)
C(28)	41(3)	65(4)	41(4)	23(3)	10(3)	15(3)
C(29)	49(4)	72(4)	52(4)	34(4)	24(3)	28(3)
C(30)	43(4)	62(4)	52(4)	28(3)	19(3)	22(3)
C(31)	37(3)	50(3)	49(4)	19(3)	10(3)	14(3)
C(32)	48(4)	65(4)	65(5)	18(4)	23(4)	21(3)
C(33)	47(4)	52(4)	84(6)	10(4)	18(4)	21(3)
C(34)	48(4)	55(4)	95(6)	27(4)	19(4)	16(3)
C(35)	51(4)	78(5)	63(5)	34(4)	8(4)	17(4)
C(36)	44(4)	69(4)	46(4)	26(3)	9(3)	11(3)
C(37)	48(4)	53(4)	45(4)	20(3)	19(3)	17(3)
C(38)	52(4)	55(4)	46(4)	20(3)	24(3)	20(3)
C(39)	46(4)	45(3)	60(4)	21(3)	20(3)	18(3)
C(40)	36(3)	66(4)	57(4)	37(4)	15(3)	19(3)
C(41)	59(4)	79(5)	47(4)	33(4)	30(4)	33(4)
C(42)	55(4)	49(3)	55(4)	27(3)	26(3)	20(3)
C(43)	39(3)	55(4)	53(4)	24(3)	16(3)	12(3)
C(44)	40(3)	63(4)	54(4)	27(3)	17(3)	17(3)

C(45)	46(4)	72(5)	62(5)	24(4)	24(4)	14(3)
C(46)	55(4)	75(5)	65(5)	20(4)	10(4)	29(4)
C(47)	52(4)	60(4)	66(5)	31(4)	9(4)	22(3)
C(48)	39(3)	63(4)	61(4)	33(4)	13(3)	17(3)
C(49)	47(4)	55(4)	59(4)	37(3)	24(3)	18(3)
C(50)	43(4)	85(5)	43(4)	25(3)	11(3)	27(4)
C(51)	50(4)	114(7)	69(6)	47(5)	22(4)	30(5)
C(52)	38(4)	99(6)	72(5)	39(5)	21(4)	20(4)
C(53)	62(5)	72(5)	56(4)	26(4)	32(4)	26(4)
C(54)	49(4)	69(4)	50(4)	29(3)	20(3)	23(3)

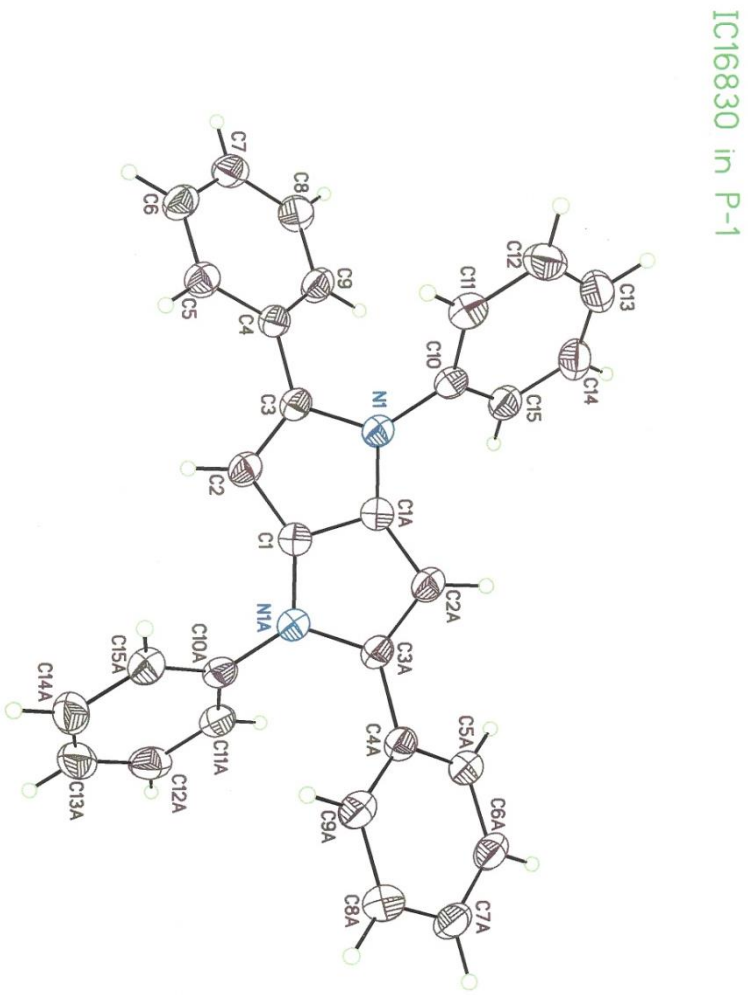

Figure S8 The ORTEP of **4**

Table S6. Crystal data and Structure refinement for 4 (number ic16830)

Crystal data and structure refinement for ic16830.

Identification code	ic16830
Empirical formula	$C_{30}H_{22}N_2$
Formula weight	410.50
Temperature	295(2) K
Wavelength	1.54178 Å
Crystal system	Triclinic
Space group	$P\bar{1}$
Unit cell dimensions	a = 6.1843(15) Å alpha = 95.690(15)° b = 7.4512(13) Å beta = 95.670(18)° c = 11.960(2) Å gamma = 100.847(18)°
Volume, Z	534.70(19) $Å^3$, 1
Density (calculated)	1.275 Mg/m^3
Absorption coefficient	0.572 mm^{-1}
F(000)	216
Crystal size	0.20 x 0.15 x 0.10 mm
Θ range for data collection	3.74 to 67.96°
Limiting indices	$-7 \le h \le 5$, $-8 \le k \le 8$, $-13 \le l \le 14$
Reflections collected	3060
Independent reflections	1933 (R_{int} = 0.0507)
Completeness to Θ = 67.96°	99.0 %
Absorption correction	Semi-empirical from equivalents
Max. and min. transmission	1.00000 and 0.47846
Refinement method	Full-matrix least-squares on F^2
Data / restraints / parameters	1933 / 0 / 145
Goodness-of-fit on F^2	1.082
Final R indices [I>2σ(I)]	R1 = 0.0798, wR2 = 0.2003
R indices (all data)	R1 = 0.1229, wR2 = 0.2340
Largest diff. peak and hole	0.287 and -0.211 $eÅ^{-3}$

Table S7. Atomic coordinates for 4 (number ic16830)

Atomic coordinates [x 10^4] and equivalent isotropic displacement parameters [$Å^2$ x 10^3] for ic16830. U(eq) is defined as one third of the trace of the orthogonalized U_{ij} tensor.

	x	y	z	U(eq)
N(1)	904(5)	67(4)	8684(3)	53(1)
C(1)	463(6)	484(5)	10522(3)	53(1)
C(2)	2454(6)	1660(5)	10366(3)	56(1)
C(3)	2715(6)	1388(5)	9254(3)	52(1)
C(4)	4459(6)	2381(5)	8646(3)	52(1)
C(5)	6646(6)	2819(5)	9162(3)	57(1)
C(6)	8291(6)	3774(6)	8624(4)	62(1)
C(7)	7816(7)	4287(6)	7573(4)	68(1)
C(8)	5650(8)	3884(6)	7057(4)	70(1)
C(9)	3979(7)	2931(6)	7596(4)	66(1)
C(10)	609(6)	-787(5)	7547(3)	53(1)
C(11)	2227(7)	-1636(6)	7124(4)	65(1)
C(12)	1905(9)	-2468(7)	6023(4)	78(1)
C(13)	-67(9)	-2484(7)	5348(4)	79(1)
C(14)	-1650(8)	-1671(6)	5765(4)	73(1)
C(15)	-1325(7)	-811(6)	6864(3)	63(1)

Table S8. Bond lengths and angles for 4 (number ic16830)

Bond lengths [Å] and angles [°] for ic16830.

N(1)-C(1)#1	1.375(5)	N(1)-C(3)	1.410(4)
N(1)-C(10)	1.422(5)	C(1)-N(1)#1	1.375(5)
C(1)-C(1)#1	1.390(7)	C(1)-C(2)	1.410(5)
C(2)-C(3)	1.355(5)	C(3)-C(4)	1.483(5)
C(4)-C(9)	1.381(6)	C(4)-C(5)	1.395(5)
C(5)-C(6)	1.379(6)	C(6)-C(7)	1.370(7)
C(7)-C(8)	1.384(6)	C(8)-C(9)	1.391(6)
C(10)-C(15)	1.376(6)	C(10)-C(11)	1.390(6)
C(11)-C(12)	1.377(6)	C(12)-C(13)	1.391(7)
C(13)-C(14)	1.354(7)	C(14)-C(15)	1.382(6)

C(1)#1-N(1)-C(3)	107.2(3)	C(1)#1-N(1)-C(10)	123.6(3)
C(3)-N(1)-C(10)	128.6(3)	N(1)#1-C(1)-C(1)#1	108.2(4)
N(1)#1-C(1)-C(2)	143.8(4)	C(1)#1-C(1)-C(2)	108.0(4)
C(3)-C(2)-C(1)	107.3(3)	C(2)-C(3)-N(1)	109.3(3)
C(2)-C(3)-C(4)	128.3(3)	N(1)-C(3)-C(4)	122.2(3)
C(9)-C(4)-C(5)	118.8(4)	C(9)-C(4)-C(3)	122.1(4)
C(5)-C(4)-C(3)	119.1(4)	C(6)-C(5)-C(4)	120.2(4)
C(7)-C(6)-C(5)	120.9(4)	C(6)-C(7)-C(8)	119.6(4)
C(7)-C(8)-C(9)	119.9(4)	C(4)-C(9)-C(8)	120.6(4)
C(15)-C(10)-C(11)	119.5(4)	C(15)-C(10)-N(1)	119.6(4)
C(11)-C(10)-N(1)	120.9(4)	C(12)-C(11)-C(10)	120.0(4)
C(11)-C(12)-C(13)	119.5(5)	C(14)-C(13)-C(12)	120.4(4)
C(13)-C(14)-C(15)	120.4(5)	C(10)-C(15)-C(14)	120.2(4)

Symmetry transformations used to generate equivalent atoms:

#1 -x,-y,-z+2

Table S9. Anisotropic displacement parameters for 4 (number ic16830)

Anisotropic displacement parameters [$Å^2 \times 10^3$] for ic16830.
The anisotropic displacement factor exponent takes the form:
$-2\pi^2 [(ha^*)^2 U_{11} + ... + 2hka^*b^* U_{12}]$

	U11	U22	U33	U23	U13	U12
N(1)	51(2)	55(2)	50(2)	7(1)	7(1)	-1(1)
C(1)	52(2)	54(2)	51(2)	5(2)	8(2)	7(2)
C(2)	56(2)	47(2)	62(2)	8(2)	7(2)	-2(2)
C(3)	49(2)	45(2)	58(2)	4(2)	8(2)	-1(2)
C(4)	52(2)	45(2)	56(2)	1(2)	10(2)	2(2)
C(5)	55(2)	53(2)	61(2)	7(2)	8(2)	6(2)
C(6)	49(2)	54(2)	78(3)	0(2)	11(2)	-2(2)
C(7)	68(3)	51(2)	77(3)	-1(2)	27(2)	-9(2)
C(8)	78(3)	64(2)	63(2)	16(2)	13(2)	-2(2)
C(9)	56(2)	68(2)	67(3)	11(2)	4(2)	-7(2)
C(10)	55(2)	47(2)	55(2)	9(2)	13(2)	-1(2)
C(11)	59(2)	64(2)	69(2)	8(2)	16(2)	1(2)
C(12)	91(3)	66(3)	77(3)	4(2)	38(3)	7(2)
C(13)	106(4)	63(2)	56(2)	-2(2)	14(3)	-9(3)
C(14)	82(3)	66(2)	60(3)	5(2)	-4(2)	-5(2)
C(15)	60(2)	61(2)	63(2)	9(2)	6(2)	-1(2)

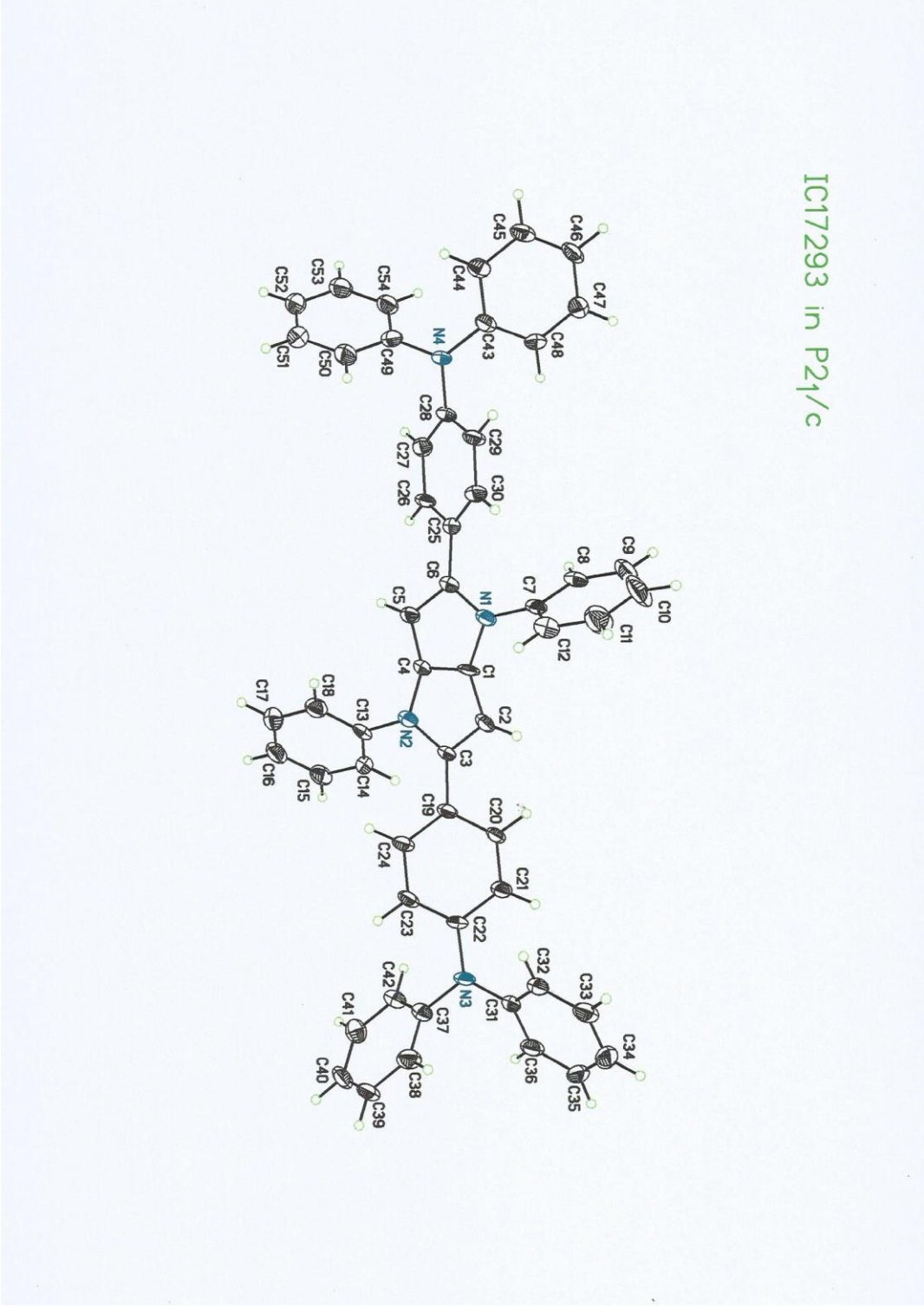

Figure S9 The ORTEP of **1**

Table S10. Crystal data and Structure refinement for 1 (number 17293)

Crystal data and structure refinement for ic17293.

Identification code	ic17293
Empirical formula	$C_{61}H_{48}N_4$
Formula weight	837.03
Temperature	150(2) K
Wavelength	0.71073 Å
Crystal system	Monoclinic
Space group	$P2_1/c$
Unit cell dimensions	a = 14.2789(13) Å alpha = 90° b = 8.5519(10) Å beta = 90.697(10)° c = 36.498(3) Å gamma = 90°
Volume, Z	4456.5(8) $Å^3$, 4
Density (calculated)	1.248 Mg/m^3
Absorption coefficient	0.073 mm^{-1}
F(000)	1768
Crystal size	0.20 x 0.15 x 0.10 mm
Θ range for data collection	3.00 to 28.35°
Limiting indices	$-18 \le h \le 18$, $-11 \le k \le 10$, $-48 \le l \le 48$
Reflections collected	29257
Independent reflections	10154 (R_{int} = 0.1924)
Completeness to Θ = 28.35°	91.1 %
Absorption correction	Semi-empirical from equivalents
Max. and min. transmission	1.00000 and 0.40315
Refinement method	Full-matrix least-squares on F^2
Data / restraints / parameters	10154 / 0 / 586
Goodness-of-fit on F^2	0.968
Final R indices [I>2σ(I)]	R1 = 0.0951, wR2 = 0.1523
R indices (all data)	R1 = 0.2733, wR2 = 0.2248
Largest diff. peak and hole	0.297 and -0.308 $eÅ^{-3}$

Table S11. Atomic coordinates for 1 (number ic17293)

Atomic coordinates [x 10^4] and equivalent isotropic displacement parameters [$Å^2$ x 10^3] for ic17293. U(eq) is defined as one third of the trace of the orthogonalized U_{ij} tensor.

	x	y	z	U(eq)
N(1)	5867(2)	2019(4)	10083(1)	27(1)
N(2)	5236(2)	3314(4)	9218(1)	27(1)
N(3)	8240(2)	4148(4)	7831(1)	28(1)
N(4)	3089(2)	1047(4)	11522(1)	27(1)
C(1)	5967(3)	2397(5)	9715(1)	26(1)
C(2)	6651(3)	2577(5)	9449(1)	28(1)
C(3)	6193(3)	3157(5)	9142(1)	23(1)
C(4)	5110(3)	2863(5)	9582(1)	25(1)
C(5)	4454(3)	2826(5)	9866(1)	25(1)
C(6)	4935(3)	2301(5)	10174(1)	26(1)
C(7)	6652(3)	1550(6)	10300(1)	27(1)
C(8)	6934(3)	2411(6)	10606(1)	34(1)
C(9)	7728(4)	1967(7)	10797(2)	51(2)
C(10)	8251(4)	717(8)	10685(2)	61(2)
C(11)	7973(4)	-119(7)	10378(2)	51(2)
C(12)	7177(3)	300(6)	10185(1)	37(1)
C(13)	4486(3)	3848(5)	8986(1)	24(1)
C(14)	4574(3)	5184(5)	8777(1)	27(1)
C(15)	3829(3)	5645(5)	8558(1)	31(1)
C(16)	3009(3)	4815(6)	8547(1)	36(1)
C(17)	2926(3)	3498(6)	8761(1)	36(1)
C(18)	3659(3)	3004(6)	8979(1)	31(1)
C(19)	6644(3)	3476(5)	8791(1)	23(1)
C(20)	7565(3)	4015(5)	8805(1)	24(1)
C(21)	8074(3)	4284(5)	8494(1)	27(1)
C(22)	7678(3)	3975(5)	8148(1)	22(1)
C(23)	6762(3)	3466(5)	8129(1)	27(1)
C(24)	6247(3)	3229(5)	8446(1)	26(1)
C(25)	4530(3)	1986(5)	10536(1)	24(1)
C(26)	3713(3)	2775(5)	10629(1)	26(1)
C(27)	3250(3)	2469(5)	10952(1)	26(1)
C(28)	3594(3)	1361(5)	11195(1)	26(1)
C(29)	4411(3)	586(5)	11108(1)	28(1)
C(30)	4862(3)	873(5)	10781(1)	27(1)
C(31)	9217(3)	3905(5)	7851(1)	24(1)
C(32)	9613(3)	2729(5)	8065(1)	29(1)
C(33)	10567(3)	2532(6)	8078(1)	34(1)
C(34)	11156(3)	3428(6)	7873(2)	36(1)
C(35)	10766(3)	4573(6)	7652(1)	35(1)
C(36)	9816(3)	4822(6)	7644(1)	31(1)
C(37)	7808(3)	4394(5)	7478(1)	26(1)
C(38)	8101(3)	3508(6)	7183(1)	33(1)
C(39)	7694(3)	3747(6)	6840(1)	36(1)
C(40)	7004(4)	4830(6)	6788(1)	37(1)
C(41)	6708(3)	5702(5)	7084(2)	35(1)
C(42)	7110(3)	5483(5)	7428(1)	30(1)
C(43)	3530(3)	998(5)	11871(1)	26(1)
C(44)	3132(3)	129(5)	12152(1)	27(1)

C(45)	3562(3)	51(6)	12492(1)	32(1)
C(46)	4392(3)	815(6)	12557(1)	33(1)
C(47)	4794(3)	1657(6)	12277(1)	34(1)
C(48)	4358(3)	1777(6)	11940(1)	31(1)
C(49)	2094(3)	982(6)	11490(1)	28(1)
C(50)	1682(3)	77(6)	11212(1)	33(1)
C(51)	722(3)	52(6)	11176(2)	40(1)
C(52)	158(3)	876(6)	11411(2)	41(2)
C(53)	565(3)	1740(6)	11687(1)	38(1)
C(54)	1523(3)	1791(5)	11727(1)	31(1)
C(55)	9475(5)	3540(9)	9639(2)	74(2)
C(56)	8789(6)	4021(11)	9886(2)	83(2)
C(57)	8387(5)	5470(12)	9887(3)	92(3)
C(58)	8697(6)	6523(10)	9616(3)	86(3)
C(59)	9380(5)	6072(9)	9368(2)	70(2)
C(60)	9774(5)	4637(10)	9375(2)	69(2)
C(61)	10502(5)	4236(9)	9115(2)	107(3)

Table S12. Bond lengths and angles for 1 (number ic17293)

Bond lengths [Å] and angles [°] for ic17293.

N(1)-C(1)	1.391(5)	N(1)-C(6)	1.397(5)
N(1)-C(7)	1.421(5)	N(2)-C(4)	1.397(5)
N(2)-C(3)	1.404(5)	N(2)-C(13)	1.433(5)
N(3)-C(31)	1.412(5)	N(3)-C(22)	1.425(5)
N(3)-C(37)	1.436(5)	N(4)-C(43)	1.414(5)
N(4)-C(49)	1.425(5)	N(4)-C(28)	1.429(5)
C(1)-C(4)	1.370(6)	C(1)-C(2)	1.394(6)
C(2)-C(3)	1.382(6)	C(3)-C(19)	1.465(6)
C(4)-C(5)	1.405(6)	C(5)-C(6)	1.387(6)
C(6)-C(25)	1.473(6)	C(7)-C(12)	1.374(6)
C(7)-C(8)	1.394(6)	C(8)-C(9)	1.377(6)
C(9)-C(10)	1.369(7)	C(10)-C(11)	1.381(7)
C(11)-C(12)	1.378(7)	C(13)-C(14)	1.380(6)
C(13)-C(18)	1.383(6)	C(14)-C(15)	1.382(6)
C(15)-C(16)	1.369(6)	C(16)-C(17)	1.377(6)
C(17)-C(18)	1.375(6)	C(19)-C(24)	1.390(6)
C(19)-C(20)	1.394(6)	C(20)-C(21)	1.375(6)
C(21)-C(22)	1.401(6)	C(22)-C(23)	1.380(6)
C(23)-C(24)	1.394(6)	C(25)-C(30)	1.386(6)
C(25)-C(26)	1.393(6)	C(26)-C(27)	1.382(6)
C(27)-C(28)	1.384(6)	C(28)-C(29)	1.381(6)
C(29)-C(30)	1.384(6)	C(31)-C(36)	1.390(6)
C(31)-C(32)	1.390(6)	C(32)-C(33)	1.372(6)
C(33)-C(34)	1.369(6)	C(34)-C(35)	1.381(7)
C(35)-C(36)	1.373(6)	C(37)-C(42)	1.375(6)
C(37)-C(38)	1.387(6)	C(38)-C(39)	1.388(7)
C(39)-C(40)	1.364(6)	C(40)-C(41)	1.383(7)
C(41)-C(42)	1.386(6)	C(43)-C(48)	1.379(6)
C(43)-C(44)	1.393(6)	C(44)-C(45)	1.380(6)
C(45)-C(46)	1.373(6)	C(46)-C(47)	1.381(6)
C(47)-C(48)	1.376(6)	C(49)-C(54)	1.382(6)
C(49)-C(50)	1.399(6)	C(50)-C(51)	1.374(6)
C(51)-C(52)	1.377(7)	C(52)-C(53)	1.374(7)
C(53)-C(54)	1.374(6)	C(55)-C(56)	1.402(9)
C(55)-C(60)	1.415(9)	C(56)-C(57)	1.366(9)
C(57)-C(58)	1.413(10)	C(58)-C(59)	1.394(9)
C(59)-C(60)	1.350(8)	C(60)-C(61)	1.457(8)

C(1)-N(1)-C(6)	107.4(4)	C(1)-N(1)-C(7)	120.9(4)
C(6)-N(1)-C(7)	131.5(4)	C(4)-N(2)-C(3)	107.4(4)
C(4)-N(2)-C(13)	123.1(4)	C(3)-N(2)-C(13)	129.4(4)
C(31)-N(3)-C(22)	120.6(4)	C(31)-N(3)-C(37)	118.8(4)
C(22)-N(3)-C(37)	120.3(4)	C(43)-N(4)-C(49)	120.4(4)
C(43)-N(4)-C(28)	122.3(4)	C(49)-N(4)-C(28)	116.8(4)
C(4)-C(1)-N(1)	107.9(4)	C(4)-C(1)-C(2)	110.6(4)
N(1)-C(1)-C(2)	141.3(4)	C(3)-C(2)-C(1)	106.0(4)
C(2)-C(3)-N(2)	109.0(4)	C(2)-C(3)-C(19)	124.4(4)
N(2)-C(3)-C(19)	126.5(4)	C(1)-C(4)-N(2)	107.0(4)
C(1)-C(4)-C(5)	109.5(4)	N(2)-C(4)-C(5)	143.2(4)
C(6)-C(5)-C(4)	106.1(4)	C(5)-C(6)-N(1)	109.0(4)
C(5)-C(6)-C(25)	126.2(4)	N(1)-C(6)-C(25)	124.6(4)
C(12)-C(7)-C(8)	120.1(5)	C(12)-C(7)-N(1)	118.7(4)
C(8)-C(7)-N(1)	121.0(4)	C(9)-C(8)-C(7)	119.2(5)
C(10)-C(9)-C(8)	120.9(5)	C(9)-C(10)-C(11)	119.6(5)
C(12)-C(11)-C(10)	120.4(5)	C(11)-C(12)-C(7)	119.8(5)

C(14)-C(13)-C(18)	120.4(4)	C(14)-C(13)-N(2)	121.2(4)
C(18)-C(13)-N(2)	118.4(4)	C(13)-C(14)-C(15)	118.8(4)
C(16)-C(15)-C(14)	121.4(4)	C(15)-C(16)-C(17)	119.2(5)
C(16)-C(17)-C(18)	120.6(5)	C(17)-C(18)-C(13)	119.6(5)
C(24)-C(19)-C(20)	117.3(4)	C(24)-C(19)-C(3)	125.7(4)
C(20)-C(19)-C(3)	117.0(4)	C(21)-C(20)-C(19)	122.2(4)
C(20)-C(21)-C(22)	120.1(4)	C(23)-C(22)-C(21)	118.5(4)
C(23)-C(22)-N(3)	122.3(4)	C(21)-C(22)-N(3)	119.2(4)
C(22)-C(23)-C(24)	120.8(4)	C(19)-C(24)-C(23)	121.1(4)
C(30)-C(25)-C(26)	117.1(4)	C(30)-C(25)-C(6)	124.7(4)
C(26)-C(25)-C(6)	118.0(4)	C(27)-C(26)-C(25)	121.8(4)
C(26)-C(27)-C(28)	120.3(4)	C(29)-C(28)-C(27)	118.5(4)
C(29)-C(28)-N(4)	122.5(4)	C(27)-C(28)-N(4)	119.0(4)
C(28)-C(29)-C(30)	121.0(4)	C(29)-C(30)-C(25)	121.3(4)
C(36)-C(31)-C(32)	117.7(4)	C(36)-C(31)-N(3)	120.2(4)
C(32)-C(31)-N(3)	122.0(4)	C(33)-C(32)-C(31)	120.3(5)
C(34)-C(33)-C(32)	122.0(5)	C(33)-C(34)-C(35)	118.0(5)
C(36)-C(35)-C(34)	120.9(5)	C(35)-C(36)-C(31)	121.0(5)
C(42)-C(37)-C(38)	119.4(5)	C(42)-C(37)-N(3)	121.4(4)
C(38)-C(37)-N(3)	119.1(4)	C(37)-C(38)-C(39)	119.6(5)
C(40)-C(39)-C(38)	121.2(5)	C(39)-C(40)-C(41)	119.0(5)
C(40)-C(41)-C(42)	120.5(5)	C(37)-C(42)-C(41)	120.2(5)
C(48)-C(43)-C(44)	118.6(5)	C(48)-C(43)-N(4)	121.5(4)
C(44)-C(43)-N(4)	119.8(4)	C(45)-C(44)-C(43)	120.5(5)
C(46)-C(45)-C(44)	120.6(5)	C(45)-C(46)-C(47)	119.0(5)
C(48)-C(47)-C(46)	120.9(5)	C(43)-C(48)-C(47)	120.4(5)
C(54)-C(49)-C(50)	119.0(4)	C(54)-C(49)-N(4)	121.5(4)
C(50)-C(49)-N(4)	119.4(4)	C(51)-C(50)-C(49)	119.2(5)
C(50)-C(51)-C(52)	121.5(5)	C(53)-C(52)-C(51)	119.1(5)
C(54)-C(53)-C(52)	120.4(5)	C(53)-C(54)-C(49)	120.8(5)
C(56)-C(55)-C(60)	117.6(8)	C(57)-C(56)-C(55)	124.4(8)
C(56)-C(57)-C(58)	116.2(8)	C(59)-C(58)-C(57)	120.5(8)
C(60)-C(59)-C(58)	122.2(8)	C(59)-C(60)-C(55)	119.2(7)
C(59)-C(60)-C(61)	120.1(8)	C(55)-C(60)-C(61)	120.8(8)

Symmetry transformations used to generate equivalent atoms:

Table S13. Anisotropic displacement parameters for 1 (number ic17293)

Anisotropic displacement parameters [$Å^2 \times 10^3$] for ic17293.

The anisotropic displacement factor exponent takes the form:

$-2\pi^2 [(ha^*)^2 U_{11} + ... + 2hka^*b^*U_{12}]$

	U11	U22	U33	U23	U13	U12
N(1)	27(2)	42(3)	13(2)	5(2)	1(2)	5(2)
N(2)	27(2)	41(3)	13(2)	3(2)	1(2)	2(2)
N(3)	27(2)	48(3)	10(2)	4(2)	6(2)	5(2)
N(4)	26(2)	45(3)	12(2)	1(2)	6(2)	-4(2)
C(1)	28(3)	40(3)	9(3)	6(2)	6(2)	5(2)
C(2)	29(3)	42(3)	12(3)	0(2)	-3(2)	3(2)
C(3)	23(3)	36(3)	10(2)	-1(2)	2(2)	0(2)
C(4)	23(3)	38(3)	13(3)	0(2)	0(2)	-2(2)
C(5)	24(3)	36(3)	17(3)	-1(2)	3(2)	3(2)
C(6)	26(3)	37(3)	13(3)	2(2)	2(2)	-1(2)
C(7)	28(3)	39(3)	14(3)	9(2)	4(2)	3(3)
C(8)	36(3)	53(3)	14(3)	-1(3)	7(2)	1(3)
C(9)	42(3)	91(5)	18(3)	-10(3)	-7(3)	9(4)
C(10)	52(4)	103(5)	28(4)	-1(4)	-18(3)	29(4)
C(11)	47(3)	71(4)	36(4)	0(3)	-4(3)	19(3)
C(12)	41(3)	45(3)	25(3)	1(3)	3(3)	0(3)
C(13)	32(3)	29(3)	10(2)	-1(2)	-1(2)	1(2)
C(14)	21(2)	38(3)	21(3)	-3(2)	1(2)	-4(2)
C(15)	37(3)	34(3)	20(3)	8(2)	-2(2)	5(3)
C(16)	36(3)	52(4)	21(3)	-2(3)	-8(2)	7(3)
C(17)	28(3)	48(3)	32(3)	-1(3)	-4(2)	1(3)
C(18)	35(3)	35(3)	22(3)	6(2)	-1(2)	2(3)
C(19)	27(3)	30(3)	12(3)	0(2)	3(2)	1(2)
C(20)	27(3)	34(3)	11(2)	0(2)	-1(2)	4(2)
C(21)	28(3)	37(3)	16(3)	4(2)	2(2)	2(2)
C(22)	29(3)	25(3)	13(3)	3(2)	7(2)	2(2)
C(23)	30(3)	38(3)	11(3)	-4(2)	0(2)	5(2)
C(24)	30(3)	35(3)	14(3)	0(2)	4(2)	6(2)
C(25)	20(2)	34(3)	17(3)	2(2)	1(2)	0(2)
C(26)	29(3)	39(3)	12(3)	6(2)	4(2)	2(2)
C(27)	25(3)	33(3)	22(3)	-4(2)	3(2)	3(2)
C(28)	28(3)	39(3)	11(3)	-3(2)	5(2)	-2(2)
C(29)	31(3)	40(3)	13(3)	4(2)	5(2)	5(3)
C(30)	27(3)	35(3)	19(3)	-1(2)	8(2)	1(2)
C(31)	23(3)	35(3)	14(3)	-6(2)	1(2)	2(2)
C(32)	28(3)	42(3)	17(3)	-1(2)	2(2)	4(3)
C(33)	41(3)	40(3)	21(3)	-4(3)	3(3)	5(3)
C(34)	26(3)	46(3)	36(3)	-14(3)	4(3)	3(3)
C(35)	29(3)	47(3)	28(3)	-12(3)	10(2)	-5(3)
C(36)	37(3)	39(3)	16(3)	2(2)	6(2)	-2(3)
C(37)	33(3)	28(3)	17(3)	2(2)	1(2)	0(2)
C(38)	35(3)	36(3)	29(3)	-6(3)	7(3)	3(3)
C(39)	45(3)	47(3)	16(3)	-10(3)	5(3)	-8(3)
C(40)	47(3)	48(3)	17(3)	1(3)	-8(3)	-13(3)
C(41)	36(3)	33(3)	34(3)	3(3)	-7(3)	2(3)
C(42)	40(3)	32(3)	17(3)	-1(2)	1(2)	1(3)
C(43)	29(3)	33(3)	16(3)	3(2)	1(2)	3(2)
C(44)	31(3)	30(3)	21(3)	-4(2)	6(2)	4(2)

C(45)	38(3)	41(3)	17(3)	2(2)	7(2)	5(3)
C(46)	38(3)	46(3)	15(3)	0(2)	-5(2)	3(3)
C(47)	34(3)	41(3)	27(3)	1(3)	-3(3)	-9(3)
C(48)	30(3)	45(3)	18(3)	3(2)	7(2)	-6(3)
C(49)	27(3)	35(3)	23(3)	5(2)	6(2)	-1(3)
C(50)	35(3)	41(3)	23(3)	-5(3)	2(2)	-1(3)
C(51)	36(3)	53(4)	30(3)	1(3)	0(3)	-12(3)
C(52)	21(3)	73(4)	30(3)	8(3)	0(3)	0(3)
C(53)	33(3)	55(4)	26(3)	4(3)	3(3)	2(3)
C(54)	33(3)	40(3)	20(3)	-1(2)	1(2)	3(3)
C(55)	76(5)	86(6)	59(5)	14(5)	-21(4)	-18(5)
C(56)	75(5)	113(7)	60(6)	1(5)	-10(5)	-18(5)
C(57)	64(5)	123(8)	89(7)	-16(6)	-23(5)	7(6)
C(58)	82(6)	85(6)	92(7)	-13(6)	-28(5)	25(5)
C(59)	76(5)	64(5)	69(6)	-4(4)	-32(4)	-2(4)
C(60)	58(4)	96(6)	53(5)	-6(5)	-21(4)	-15(5)
C(61)	83(5)	150(8)	88(7)	-30(6)	29(5)	-12(6)

Cyclic voltammetry and differential pulse voltammetry studies 1-4 and TPA

To evaluate the electrochemical properties of **1-4**, cyclic voltammetry (CV) and differential pulse voltammetry (DPV) were adopted as tool in this study. In these measurements, palladium disk electrode was employed as the working electrode, a silver/silver chloride couple was used reference electrode, and a platinum wire as the auxiliary electrode. In the electrochemical oxidation scans, dried methylene chloride was used as the solvent. Tetrabutylammonium perchlorate (TBAP), with concentration of 0.1 M, was used as the supporting electrolyte. Ferrocene was used as the internal reference for calibration of the applied electrical potential. The concentrations of **1-4** were kept at 1 x 10^{-3} M. For the anodic scans, the oxidation waves and E^{ox} were recorded with a scan rate of 100 mV/s. On the other hand, in the reduction potential (E^{re}) measurements, the cathodic scans were performed in dimethylformamide (DMF), using TBAP (0.1 M) as the supporting electrolytes, and glassy carbon electrode as the working electrode. The scan rate was set at 100 mV/s. The concentrations of **1-4** were again kept at 1 x 10^{-3} M. To exclude oxygen from the system, the solution was purged with nitrogen to 10 minutes before each electrochemical measurement.

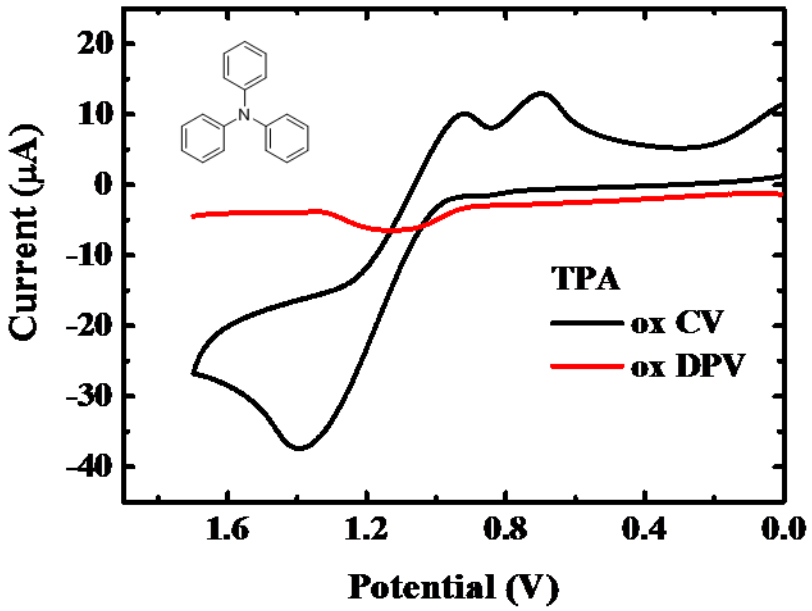

Figure S10 CV and DPV of TPA.

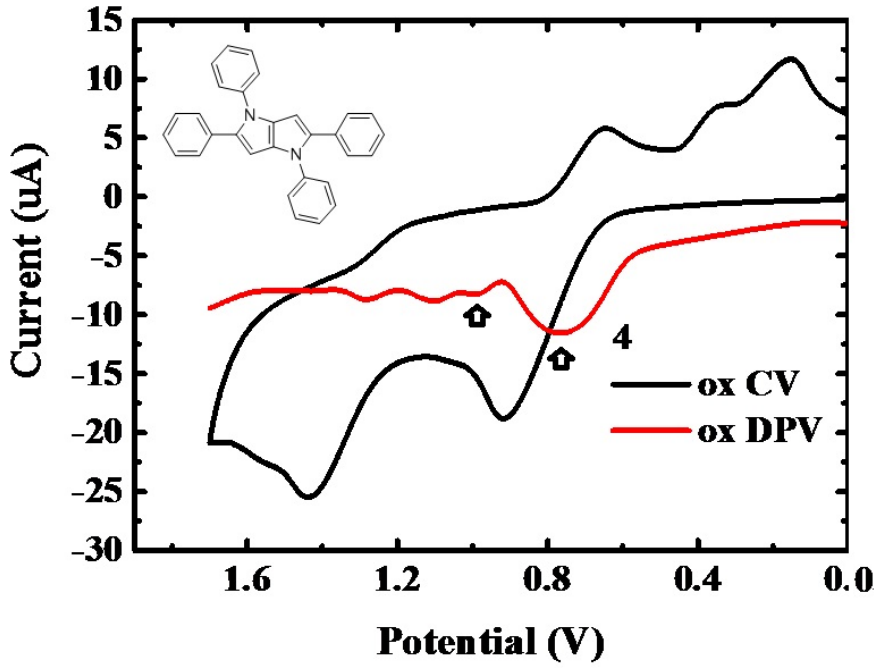

Figure S11 CV and DPV of **4.** The DPV experiment clearly demonstrated that the second wave indeed contains many different oxidation processes.

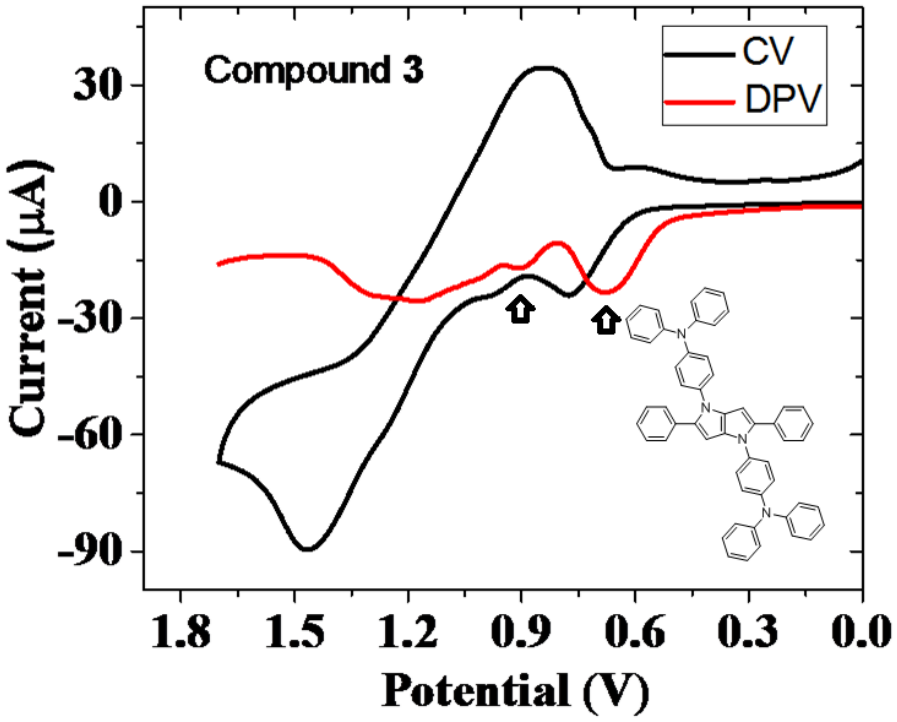

Figure S12 CV and DPV of **3**. The earlier part of oxidation wave pattern of **3** is very similar to that of **4**, indicating that the electronic coupling between the TPA units and the DHPP core is weak

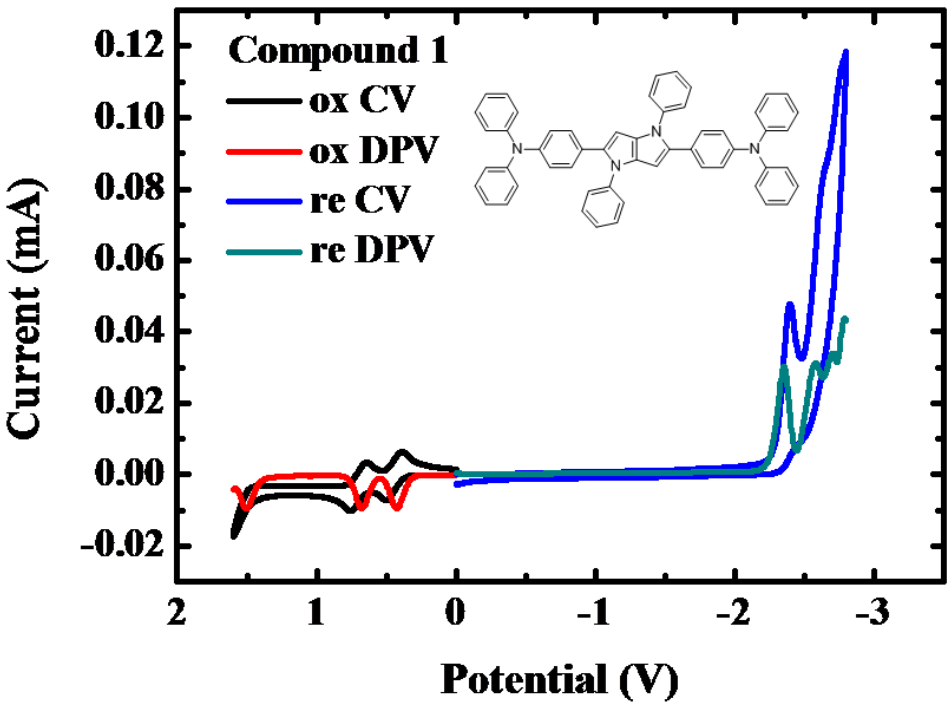

Figure S13 CV and DPV of **1**. The oxidation pattern is dramatically different from that of **3** and **4**. To reversible waves are shown at 0.3-0.7 V, indicating that oxidations at the DHPP core are strongly stabilized by the TPA units at the 2,5- positions.

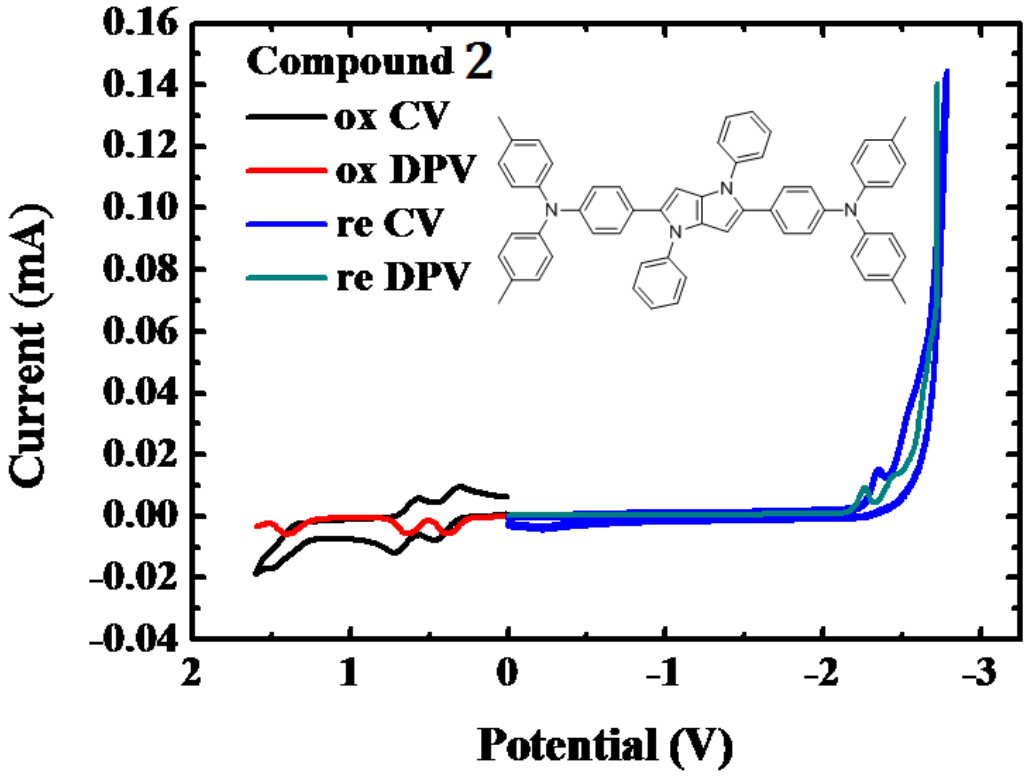

Figure S14 CV and DPV of **2**. Nearly identical patterns with **1** are observed.

Table S14. Photophysical properties of DHPP 1-4 and Triphenylamine

compound	λ_{max}^{Abs} (nm)	λ_{max}^{FL} (nm)	λ_{max}^{LTFL} (nm)	Stokes shift (nm)	Q.Y.[a]
1	380 (ε =72100 $M^{-1}cm^{-1}$)	448	436	68	0.63
2	384 (ε =60800 $M^{-1}cm^{-1}$)	451	439	67	0.71
3	343 (ε =71800 $M^{-1}cm^{-1}$)	407	400	64	0.57
4	350 (ε =44900 $M^{-1}cm^{-1}$)	404	391	54	0.67
TPA	295 (-)	360	358	65	-

a. coumarin 1 (Q.Y. = 0.85) [3,4] in 2-MeTHF is used as reference for fluorescence quantum yield measurements.

Preliminary studies of photochromic response of 1 in the presence of various halocarbons

Preliminary photochromic responses of **1** (1 x 10^{-5}) with additional halocarbons other than those reported in the article indeed have been tested. Their color changse are shown in the following picture (Figure S15). From left to right are $CHCl_3$; $Cl(CH_2)_3Cl$; $Br(CH_2)_3Br$; $I(CH_2)_3I$ in toluene, 1,4-$C_6H_4I_2$ in toluene; $CHBr_3$; *n*-hexBr; 1,2-$C_6H_4Cl_2$, 1,2-$BrC_6H_4NO_2$ in toluene; 1,4-$ClC_6H_4NO_2$ in toluene; 1,4-$FC_6H_4NO_2$ in toluene; $C_6H_5NO_2$. It is noteworthy to mention that most of the aromatic halides are less sensitive. Introducing nitro group onto the aromatic ring does not help to facilitate the photochromic response, which is reasonable. It is simply because the PET in these cases does not trigger any C-X bond dissociation. Reminded that in our mechanisms, , the PET process has to transfer an electron to the C-X^* antibonding orbital to trigger the C-X bond dissociation. The presence of a nitro substitutient provides a low lying LUMO. PET from **1** to the LUMO of the NO_2 substituent does not lead to any fruitful photochromic results.

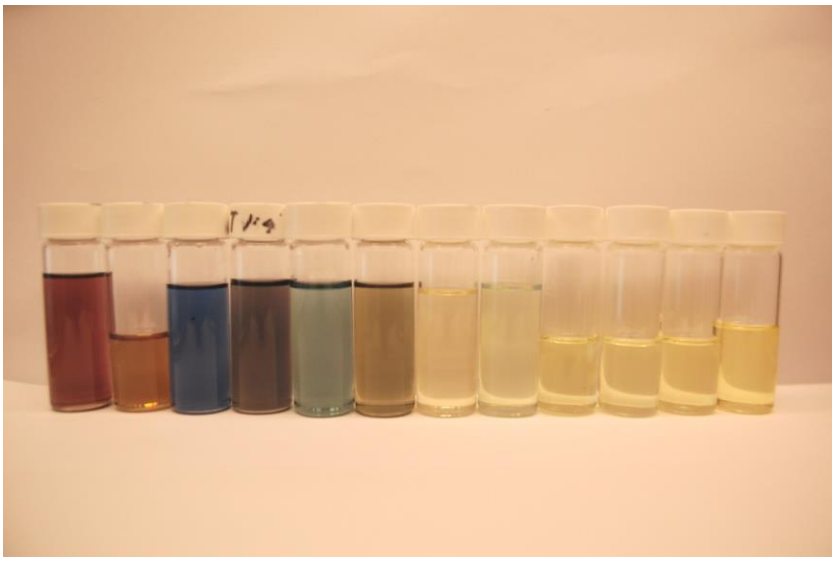

Figure S15. Photochromic responses of **1** (1 x 10^{-5} M) with additional halocarbons other than those reported in the article indeed have been tested. Their color changse are shown in the following picture. From left to right are $CHCl_3$; $Cl(CH_2)_3Cl$; $Br(CH_2)_3Br$; $I(CH_2)_3I$ in toluene, 1,4-$C_6H_4I_2$ in toluene; $CHBr_3$; n-hexBr; 1,2-$C_6H_4Cl_2$, 1,2-$BrC_6H_4NO_2$ in toluene; 1,4-$ClC_6H_4NO_2$ in toluene; 1,4-$FC_6H_4NO_2$ in toluene; $C_6H_5NO_2$.

Time resolved photochromic studies.

UV fluorescence lamp (366 nm), with the calibrated output intensity of 1 mw/cm^2, was used as the light source for photo-excitation. The concentration of **1** is 5 x 10^{-5} M except otherwise noted. The test clearly demonstrated that no significant color change was observed in the non-halogenated solvents. However, in the presence of halocarbons, the photochromic change is pretty obvious. The photochromic change of **1** in a solution of halocarbon (1 M) in PhMe was followed by time resolved UV-Vis spectrometric method. The data from CH_2Cl_2, $CHCl_3$, CCl_4, $Br(CH_2)_2Br$; $Br_2CHCHBr_2$, $CHBr_3$, and CH_2I_2 are summarized in Figures S16-S21. Since the efficiency of photochromic response in CH_2Cl_2 is low with only small absorbance change in the visible region (Figure S16), the kinetics will be interfered by other non-photochromic processes so that the time resolved data is hard to be conclusive . On the other hand, for $CHCl_3$, CCl_4, $Br(CH_2)_2Br$; $Br_2(CH)_2Br_2$, $CHBr_3$, the photochromic changes along with an isosbestic point are observed. Their data at 390 nm follow well the first order decay of

$$t= -\tau\cdot\ln((A -A_\infty)/(A_o-A_\infty)) \quad (1)$$

Complicated by the absorption of CH_2I_2, the absorption decay at 390 nm cannot be used as an index to reflect the reactivity. On the other hand, the photochromic change at 626 nm clearly demonstrated that the color change is originated from a multi-step process, indicating that the photochromic mechanisms are more complicated in this case (Figure S21).

(a)

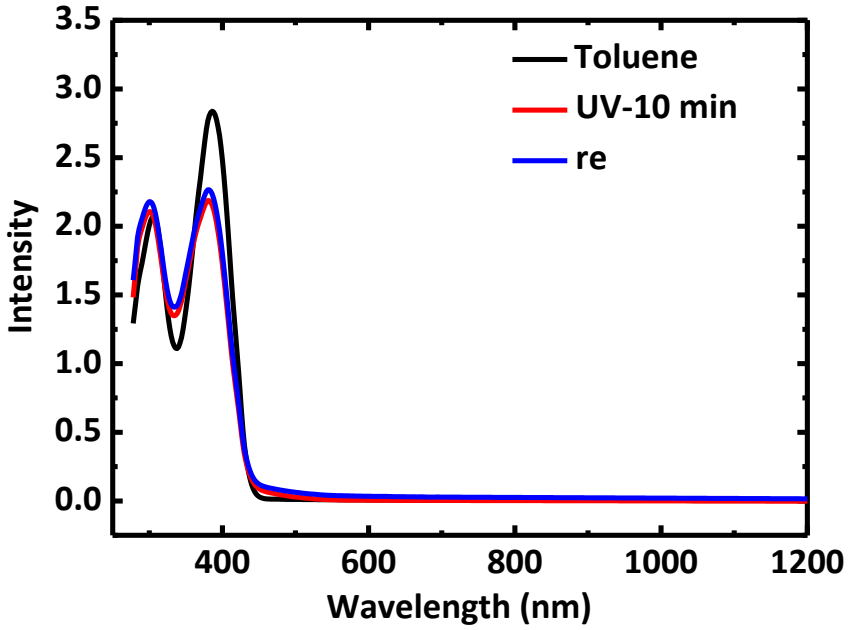

(b)

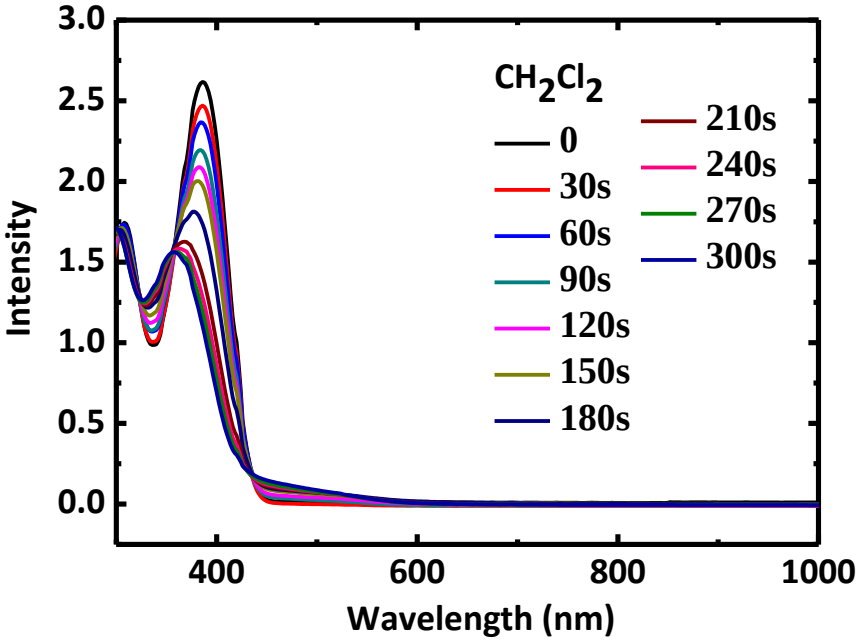

Figure S16. (a) Photochromic response of **1** in pure toluene. (b) Time resolved photochromic change of **1** in the presence of CH_2Cl_2 in Toluene (1 M). Due to the low reactivity of CH_2Cl_2. The photochromic change is similar to but slightly faster than the background change.

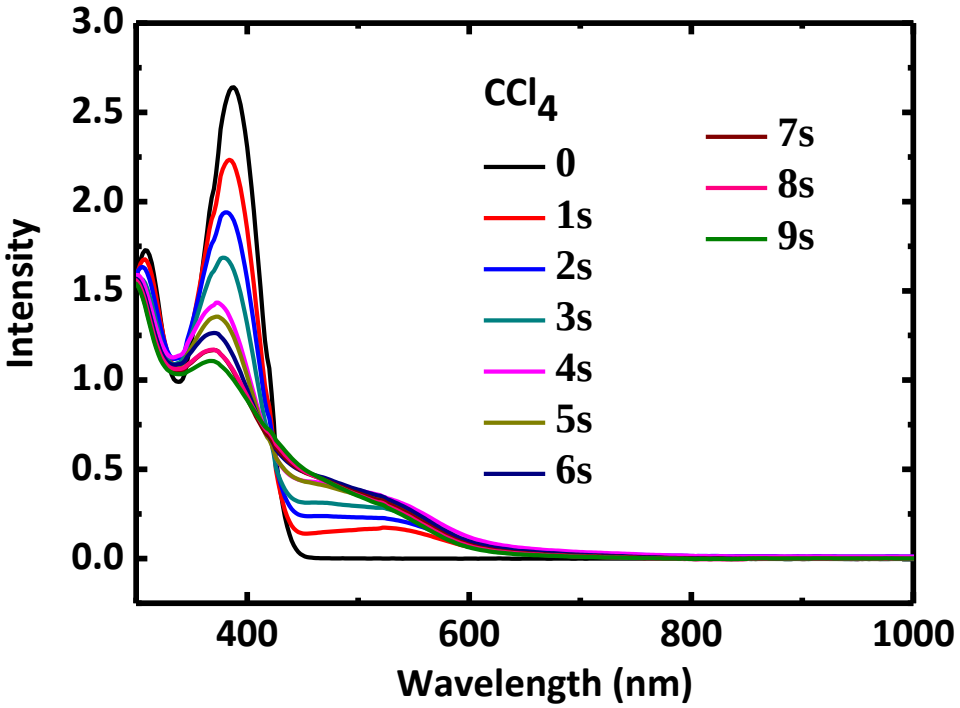

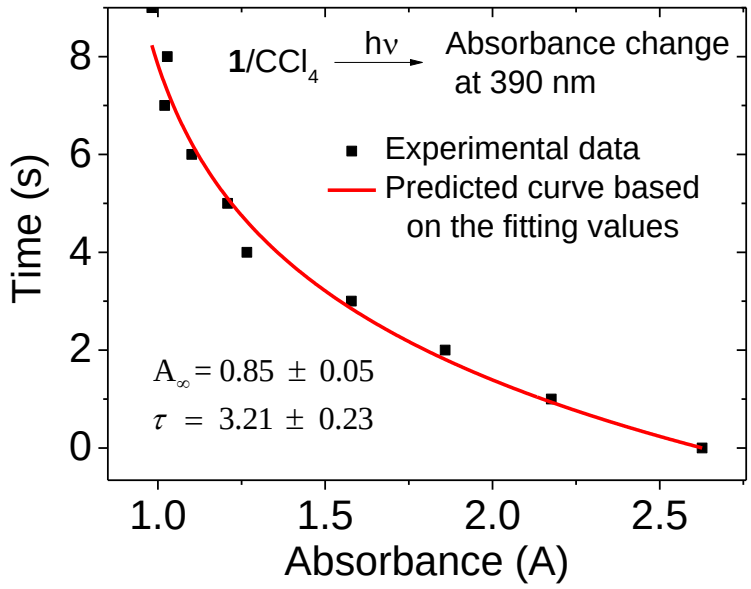

Figure S17. Time resolved photochromic change of **1** in the presence of CCl_4 in toluene

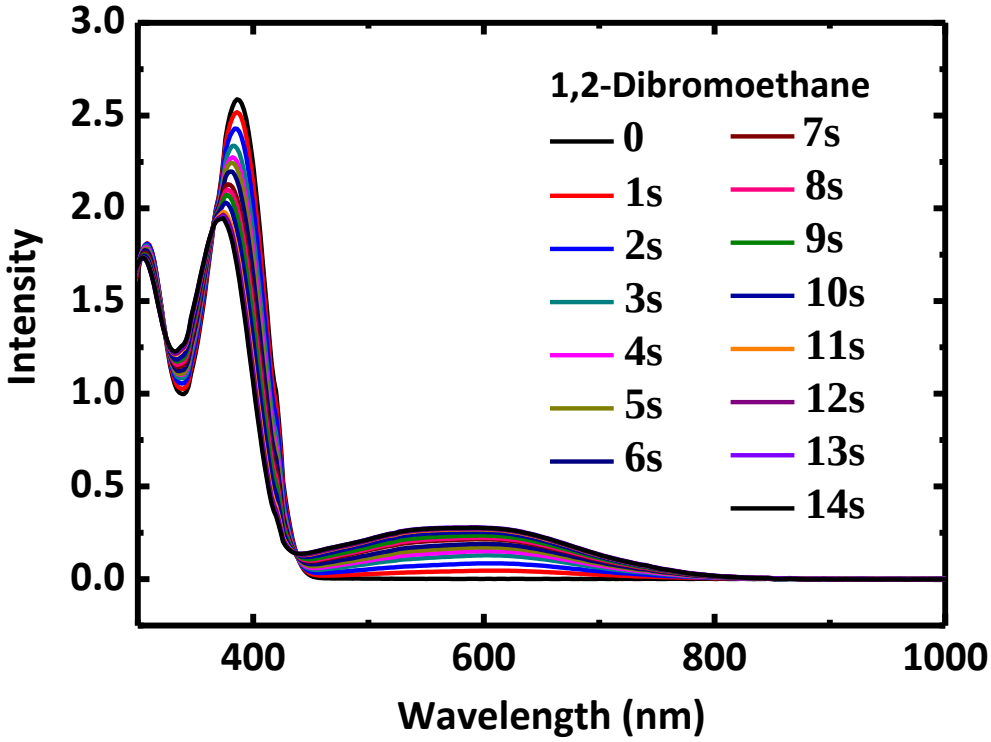

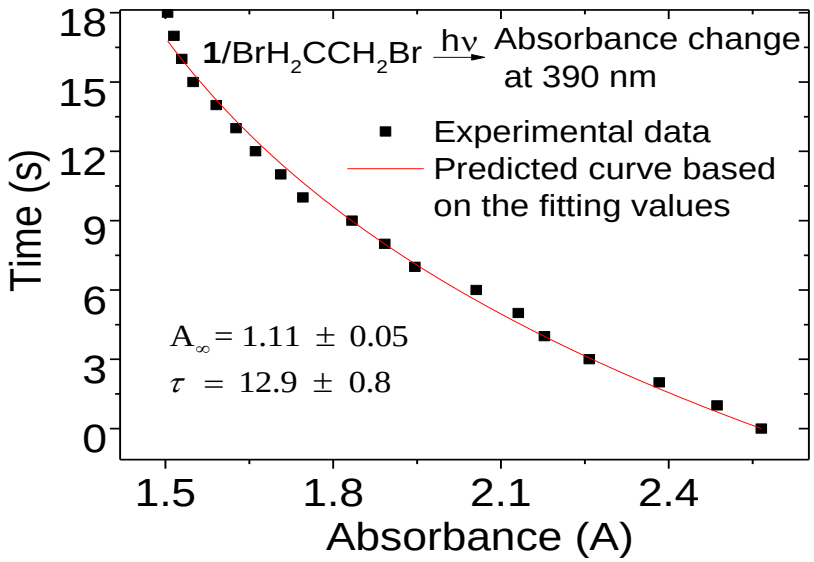

.

Figure S18. Time resolved photochromic change of **1** in the presence of $Br(CH_2)_2Br$ in toluene

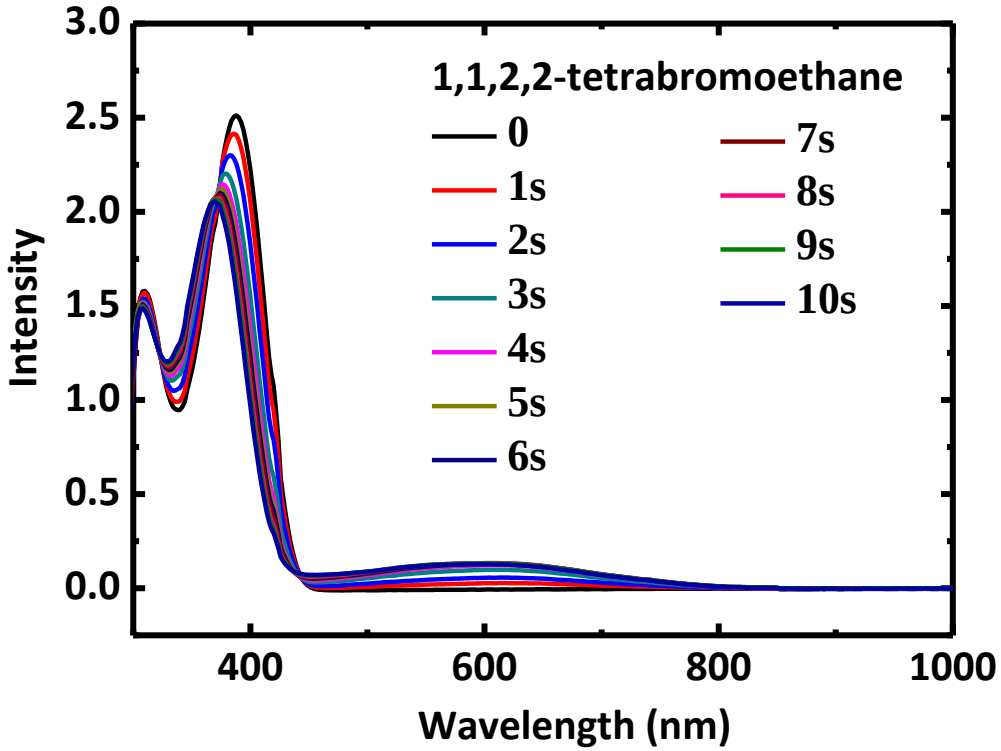

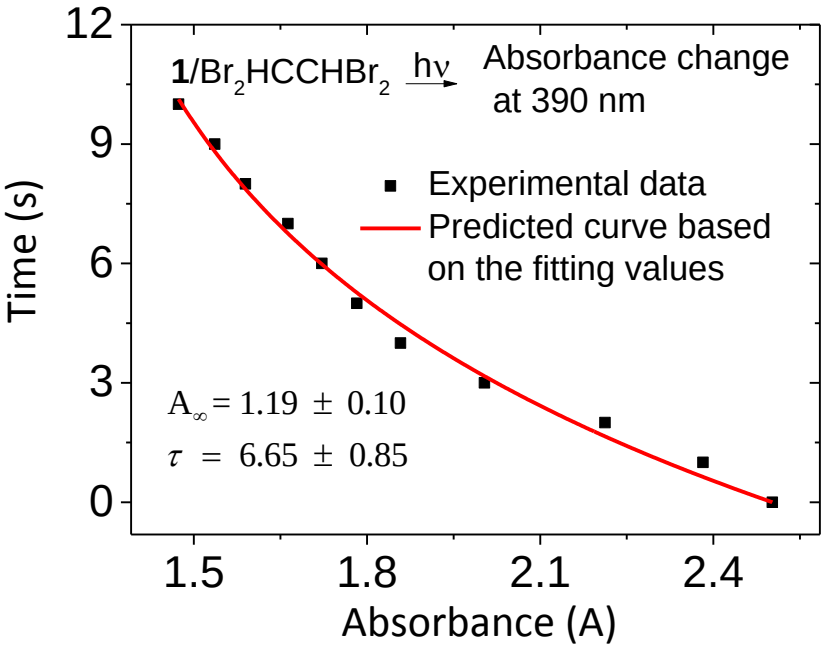

Figure S19. Time resolved photochromic change of **1** in the presence of $Br_2CHCHBr_2$ in Toluene

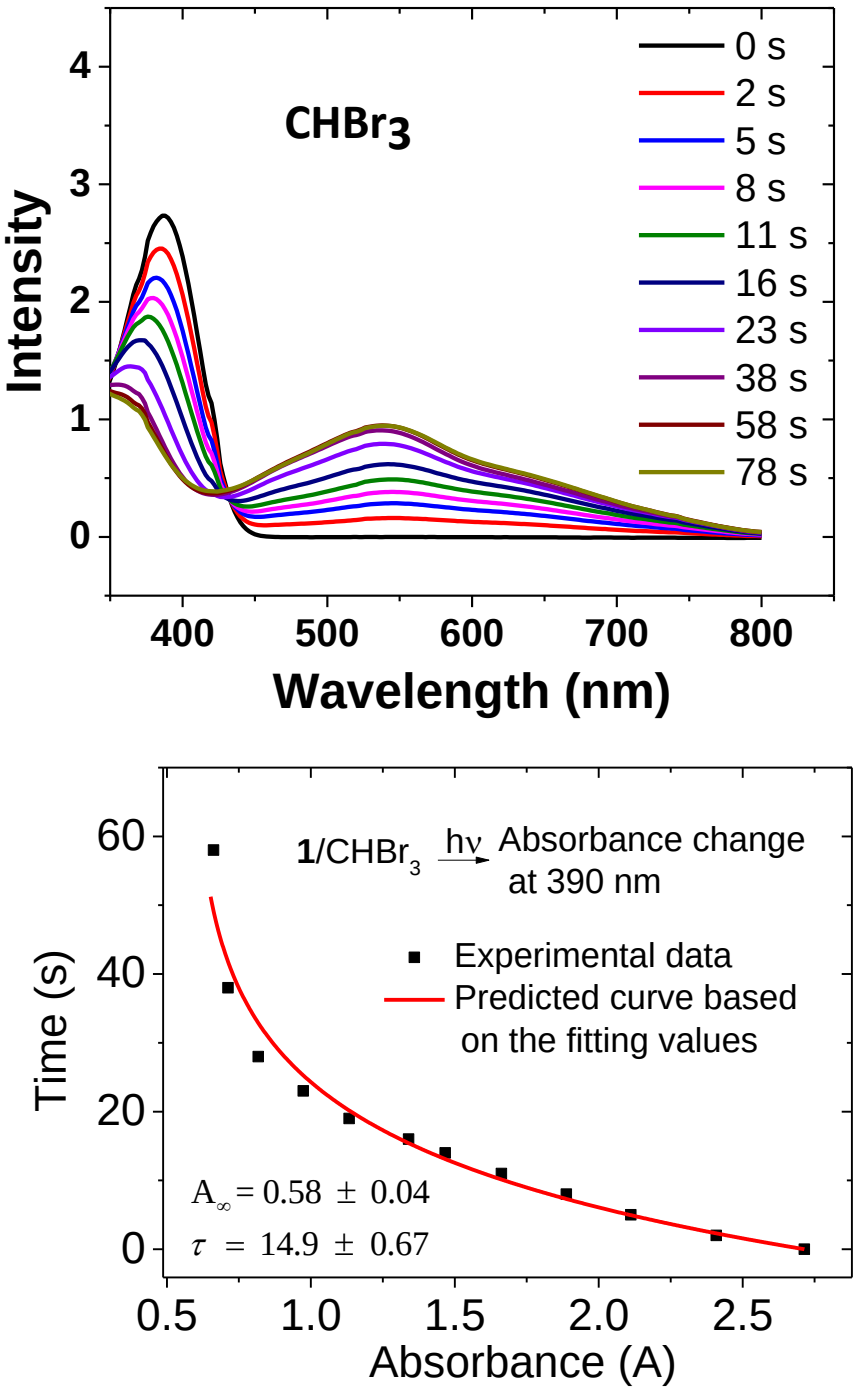

Figure S20. Time resolved photochromic change of **1** in the presence of $CHBr_3$ in Toluene

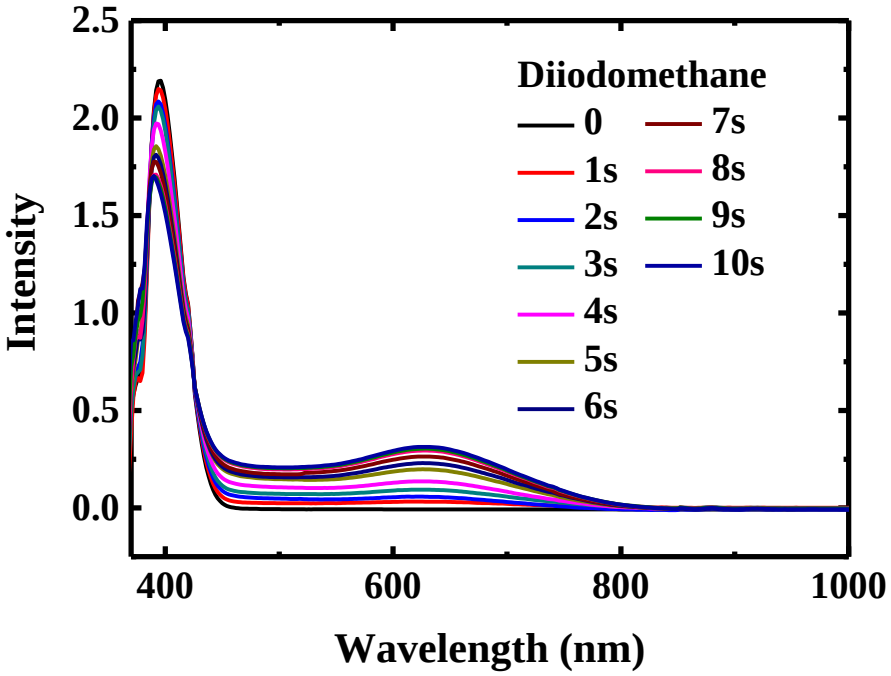

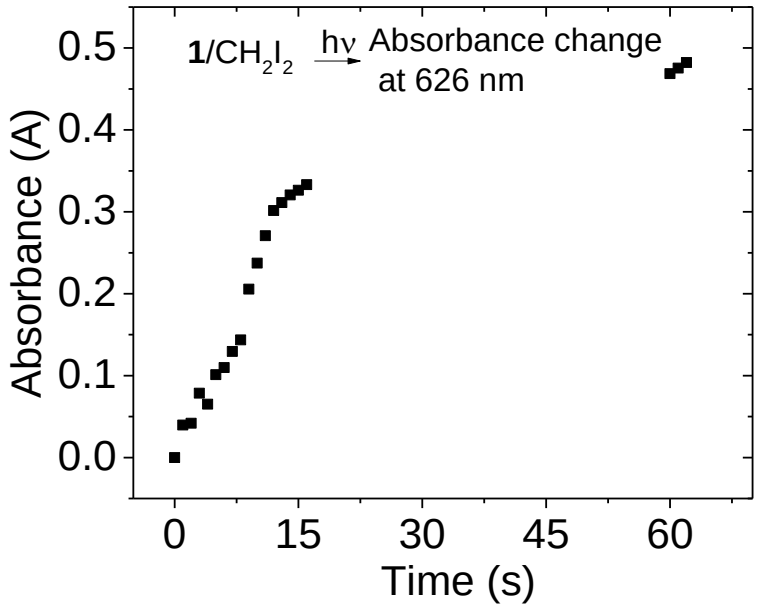

Figure S21. Time resolved photochromic change of **1** in the presence of CH_2I_2 in Toluene

Preliminary studies of the PET mechanisms.

For more in-depth understanding the PET mechanisms, we have employed spectroelectrochemical methods as tool to assist our study.

As shown in the following scheme, radical cation of **1** will be generated through PET with $CHCl_3$.

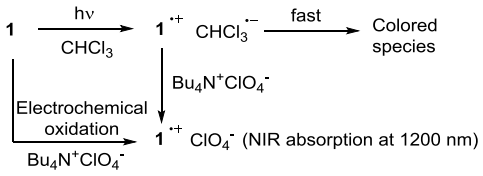

To obtain direct evidence to support our hypothesis of $\mathbf{1}^{(\cdot+)}$ formation in the PET, we have generated $\mathbf{1}^{(\cdot+)}$ by electrochemical method and obtained the absorption spectrum of $\mathbf{1}^{(\cdot+)}$ for comparison. In the spectroelectrochemical analyses, a piece of platinum gauze was used as the working electrode and auxiliary electrode, and a silver/silver chloride couple was used as the reference electrode. Dry TBAP (0.1 M) in CH_2Cl_2 was used as the supporting electrolyte. The concentrations of **1** and **2** are about 5 x 10^{-5} M and 1 x 10^{-5} M. UV-Vis-NIR absorption spectra were collected for every voltage increment of 0.1 V. (Figure S22)

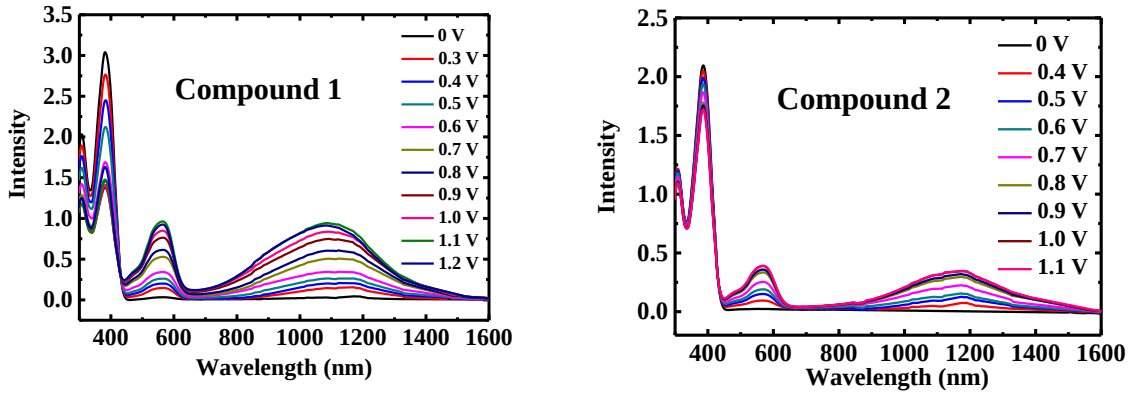

Figure S22. Spectroelectrochemical analyses of $\mathbf{1}^{(\cdot+)}$ (left) and $\mathbf{2}^{(\cdot+)}$ (right) in CH_2Cl_2, using TBAP (0.1 M) as the supporting electrolyte.

The spectral absorptions peaked at 550 nm in the visible region and at 1100 nm in the NIR region began to appear at 0.3-0.4 V, indicating that these absorption is originated from the first oxidation. In addition, the presence of the NIR absorption is characteristic for the bis-triarylamine radical cation in literature, which is assigned to the intervalence charge transfer absorption.

Once we had collected the spectral identity of $\mathbf{1}^{(\cdot+)}$ at hand, we took steps forward to examine whether $\mathbf{1}^{(\cdot+)}$ exists in the photochromic process. Since $\mathbf{1}^{(\cdot+)}$ is only reactive intermediates during the photochromic process, the concentration should be low. Fortunately, the absorption of $\mathbf{1}^{(\cdot+)}$ in the NIR region can still be observed, even though their absorbance is very low. At the early stage of the photochromic process, or under irradiation by fluorescent lamp, NIR absorption growth can be observed. The photochromic change is so sensitive that even simple fluorescence lamp can slowly induce color change. However, the NIR absorption gradually dropped and disappeared after prolonged illumination for 5 s.

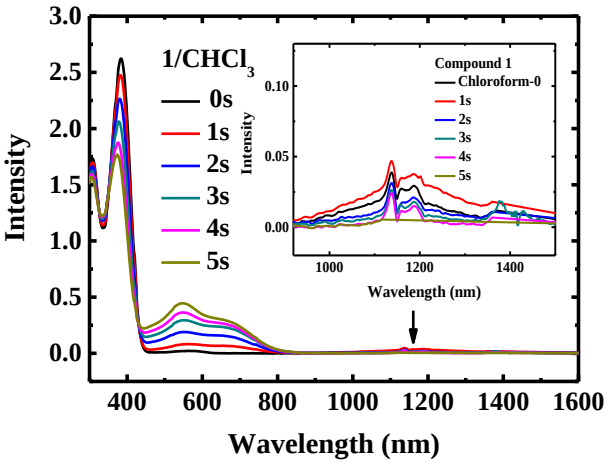

Figure S23. Time resolved photochromic change of **1** in the presence of $CHCl_3$ in Toluene.

Although the radical cation intermediate $\mathbf{1}^{(\cdot+)}$ may be decompose quickly under normal conditions, we might be able to trap the $\mathbf{1}^{(\cdot+)}$ by using counter ion exchange to form $\mathbf{1}^{(\cdot+)}/ClO_4^-$, which prohibits it from further reaction with $C\text{-}X^{(\cdot-)}$. In these case, **1** and **2** (5×10^{-5} M) in

$CHCl_3$ or in CH_2Cl_2 were irradiated in the presence of Bu_4NClO_4 (1×10^{-3} M), and a clear-cut additional NIR signal peaking at 1100 nm can be snap-shoot. In $CHCl_3$ the photochromic sensitivity of **1** and **2** is so high that, as shown in Figure S24, the photochromic change occurs at 550 and 1100 nm even under fluorescence lamp illumination. This is almost identical with the characteristic absorption of $\mathbf{1}^{(\cdot+)}$ and $\mathbf{2}^{(\cdot+)}$ generated in the spectroelectrochemical experiments. NIR absorption can also be observed with CH_2Cl_2 after UV (366 nm). All these

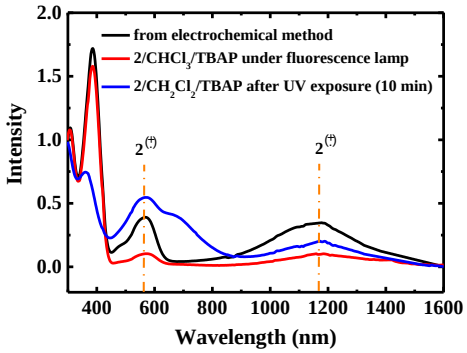

suggest the existence of the PET process in the photochromic process.

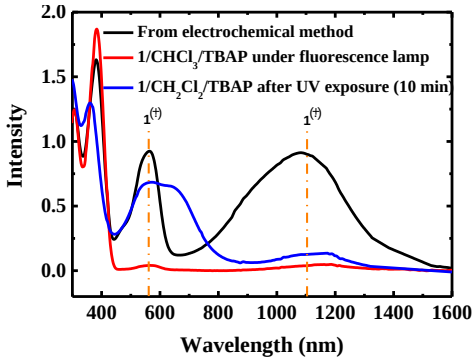

Figure S24. Photochromic change of **1** or **2** in $CHCl_3$ and in CH_2Cl_2 in the presence of Bu_4NClO_4.

Quantitative Analysis of $CHCl_3$ and CH_2Cl_2 Contents.

To establish calibration curves for the $CHCl_3$, sets of $CHCl_3$ standards with various concentrations were analyzed by DHPP at 27.0 ^oC. The mother solution of DHPP was prepared in toluene (0.01 M). The concentration of $CHCl_3$ in CH_3CN spans the range from 0.001 M to 0.1 M. In each analysis, one portion of the DHPP mother solution (0.1 mL) and one portion of $CHCl_3$ solution (0.1 mL) were mixed and diluted to 1 mL with a mixed solvent of CH_3CN and toluene (2:1). The detection limit of this method indeed can be extended to as low as 0.0001M

A fluorescence quartz cell was adopted with the optical path width of 1 mm and optical path length of 1 cm for spectrometric detection. UV light (366 nm) was irradiated from the side-way to induce the photochromic change and the color change was observed along with the direction of spectrometric detection. (Figure S25).

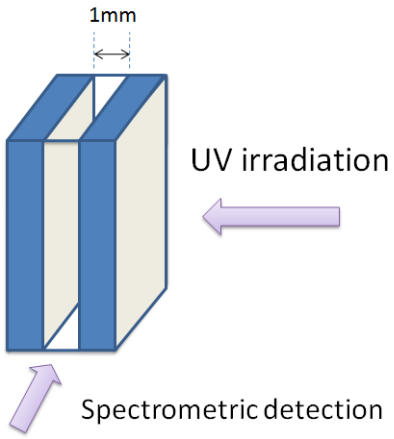

Figure S25. The cell for detection of the photochromatic change.

The photochromic response was monitored against irradiation time. The UV irradiation source was chopped during the period of spectrometric data collection so as to avoid any optical interference. The corresponding spectral changes with various concentration of $CHCl_3$ are shown in Fig S26. The reaction rate in each case of the photochromic process was obtained from their linear plot of the absorbance at 536 nm versus irradiation time. Since DHPP is photosensitive and may be oxidized under UV irradiation, photochromic change of the blank, which contains only DHPP in CH_3CN/toluene, had also been monitored and corrected.

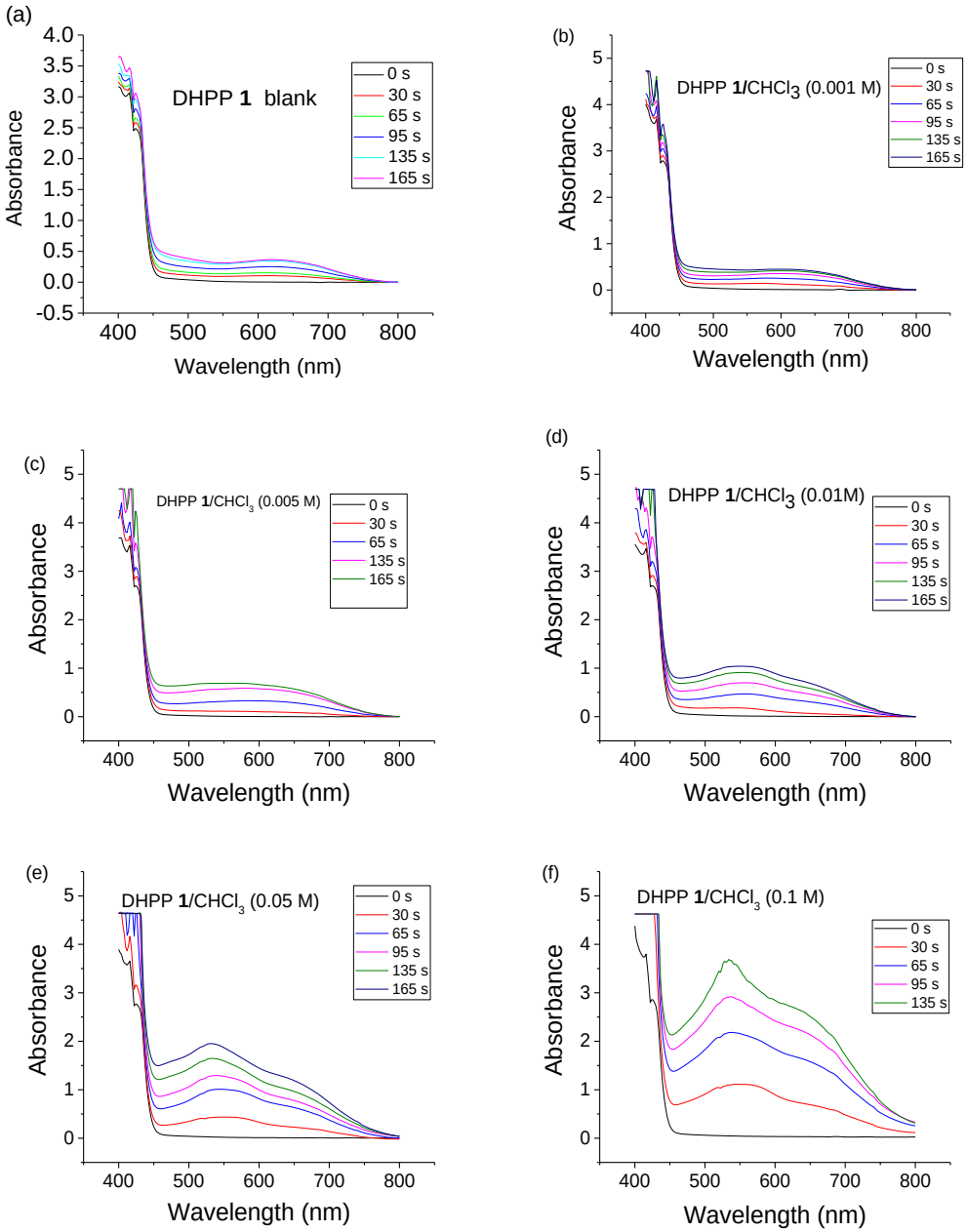

Figure S26. Photochromatic change of DHPP**1** (0.001 M) in CH_3CN/toluene (2:1) in the presence of $CHCl_3$ with the sample concentration of: (a) blank, (b) 0.001 M, (c) 0.005 M, (d) 0.01M, (e) 0.05 M, (f) 0.1M. Note that the samples were diluted by 10 times before measurement.

As shown in Figure 8 in the manuscript, the initial rate is linearly proportional to the concentration of $CHCl_3$. However, due to the limitation of Beer's law, certain deviation from the linearity was clearly observed at the high absorbance region (A>1). Therefore, for purpose of quantitative analysis of $CHCl_3$, the concentration should be adjusted so that the absorbance at 536 nm would fall into the range between 0.01-1.0.

Linear plots of the absorbance change against irradiation time in the presence of various concentrations of $CHCl_3$ were first obtained. The slope of each line representing the rate of photochromic change was then obtained from the plot. Inset Figure 8 in the manuscript shows the plot of rate of photochromic change versus [$CHCl_3$]. The observation of the linear behavior suggests a pseudo first order kinetics for [$CHCl_3$].

To simplify the calibration process, a calibration curve from the absorbance data of 536 nm at 135 s as shown in Figure 9 in the manuscript, with the corresponding [$CHCl_3$] at 0.001, 0.005, and 0.01 M, were established for analysis. After background correction, a linear calibration plot can be clearly observed. The method detection limit (> 2.6 σ from zero) can be as low as 100 ± 28 ppm. The error estimations are based on the average and standard deviations from several times of independent experiments. The experimental uncertainty ΔA in the absorbance (A) measurements is 0.02 and $\Delta A/A$ is about 27% of error. The uncertainty $\Delta\sigma$ of the slope σ in Figure 9 is 6.2%. The error at 100 ppm is calculated as 28 ppm according to the equation of

$$\Delta R = |R| \times [(\Delta A/A)^2 + (\Delta\sigma/\sigma)^2]^{1/2} \quad (2)$$

Similar error estimation was applied for CH2Cl2 analysis

Quantitative Analysis of CH_2Cl_2 Content:

Due to the relatively low reactivity, dichloromethane can only be analyzed at a relatively high concentration (Figure S27). To secure that the results were not interfered by other higher halo-homologues, the purity of CH_2Cl_2 were further confirmed by ^1H NMR. On the basis of our analysis, the amount of $CHCl_3$ contaminant should be less than 1/10000 and the present photochromic change should arise from the photoelectron transfer reaction between **1** and CH_2Cl_2. The concentration of mother DHPP solution was 0.01 M in toluene. To a volumetric flask (2 mL) was added the mother solution of DHPP (0.2 mL), the corresponding amounts of CH_2Cl_2 (1 mL, 0.5 mL, and 0.25 mL) respectively and diluted to volume with CH_3CN. The samples were irradiated as described before. The photochromic changes were recorded and shown in Figure S27.

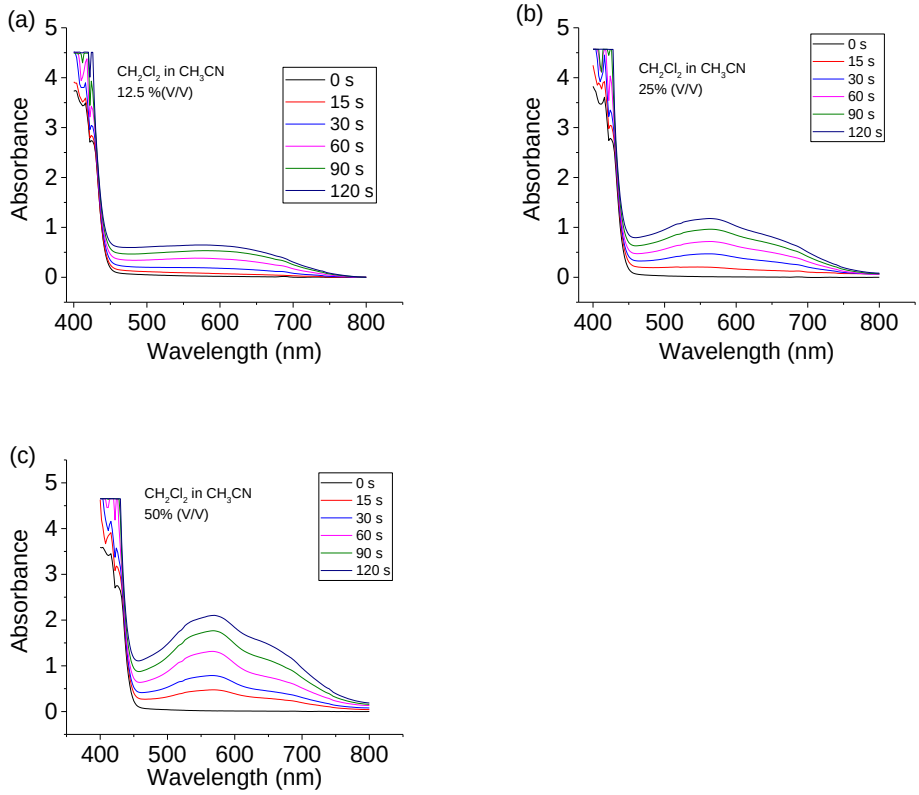

Figure S27. Photochromatic change of DHPP**1** (0.001 M) in CH_3CN/toluene (2:1) in the presence of various amounts of CH_2Cl_2: (a) 12.5 V/V%; (b) 25 V/V%;' (c) 50 V/V%.

The initial reaction rate (Figure S28) in each case of the photochromic process was obtained from their linear plot of the absorbance at 560 nm versus irradiation time. Photochromic change of the blank, which contains only DHPP in CH_3CN/toluene, had also been monitored and corrected.

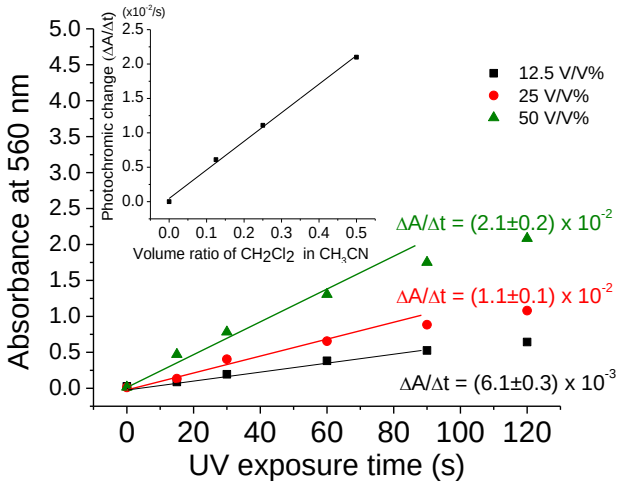

Figure S28. Linear plots of the absorbance change against irradiation time in the presence of various concentrations of CH_2Cl_2. The slope of each line represents the rate of photochromic change. Inset is the plot of the plot of rate of photochromic change versus $[CH_2Cl_2]$. The observation of the linear behavior suggests a pseudo first order kinetics for $[CH_2Cl_2]$.

As shown in the Figure 10 in the manuscript, a calibration curve from the absorbance data of 560 nm at 60 s, with the corresponding CH_2Cl_2 %(V/V) at 12.5%, 25.0% and 50.0%, was established for analysis. After background correction, a linear calibration plot can be clearly observed.

References

(1) Mayers, Brian T. and Fry, Albert J. *Org. Lett.* **2006,** *8*, 411-414.

(2) Chang, C.-W.; Chung, C.-H.; Liou, G.-S. *Macromolecules*, **2008**, *41*, 8441-8451.

(3) Rusalov, M.; Druzhinin, S.; Uzhinov, B. *J Fluoresc.* **2004**, *14*, 193-202.

(4) Williams, A. T. R.; Winfield, S. A.; Miller, J. N. *Analyst* **1983**, *108*, 1067-1071.